Research
Frontiers of Chemical Engineering—Review

Recent Developments in Hydrodynamic Cavitation Reactors: Cavitation Mechanism, Reactor Design, and Applications

Haoxuan Zheng, Ying Zheng *, Jesse Zhu

Department of Chemical and Biochemical Engineering, University of Western Ontario, London, ON N6A 3K7, Canada

ABSTRACT

Hydrodynamic cavitation is considered to be a promising technology for process intensification, due to its high energy efficiency, cost-effective operation, ability to induce chemical reactions, and scale-up possibilities. In the past decade, advancements have been made in the fundamental understanding of hydrodynamic cavitation and its main variables, which provide a basis for applications of hydrodynamic cavitation in radical-induced chemical reaction processes. Here, we provide an extensive review of these research efforts, including the fundamentals of hydrodynamic cavitation, the design of cavitation reactors, cavitation-induced reaction enhancement, and relevant industrial applications. Two types of hydrodynamic cavitation reactors—namely, stationary and rotational—are compared. The design parameters of a hydrodynamic cavitation reactor and reactor performance at the laboratory and pilot scales are discussed, and recommendations are made regarding optimal operation and geometric conditions. The commercial cavitation reactors that are currently on the market are reviewed here for the first time. The unique features of hydrodynamic cavitation have been widely applied to various chemical reactions, such as oxidization reactions and wastewater treatment, and to physical processes, such as emulsion generation and component extraction. The roles of radicals and gas bubble implosion are also thoroughly discussed.

1. Introduction

The phenomenon of cavitation was first observed and studied by Reynolds and Parsons, who examined a failure trial of a British warship in 1885. They suggested that the propeller blade was damaged as a result of an implosion of water vapor bubbles and named the phenomenon "cavitation." This phenomenon is characterized by the formation, growth, and collapse of bubbles. In the case of the warship, the collapse of cavitating bubbles was accompanied by a large amount of local energy, which caused the damage [1]. Lord Rayleigh then established the theoretical foundation for cavitation studies. Thereafter, researchers have performed extensive studies to fundamentally understand the formation of cavitation and the hydrodynamic behavior of cavitation bubbles. Most of these studies focused on how to avoid cavitation, due to its detrimental effects. However, a further understanding of cavitation encouraged researchers to explore possible approaches for making

use of the energy released by cavitation. To date, cavitation phenomena have been studied in many industrial processes, including wastewater treatment [2], the food and beverage industry [3], and biomedical applications [4].

The methodology used to generate cavitation is frequently used to define the type of cavitation. Four main types of cavitation are commonly defined: hydrodynamic, acoustic, optic, and particle cavitation. The latter two types of cavitation were discovered recently. Optic cavitation is generated by high-energy light, such as a laser. When a liquid medium is irradiated with a light, the light energy is absorbed and heats up the local liquid. If the local liquid temperature goes beyond its boiling temperature, vapor cavities/bubbles form, grow, and then collapse, in what is known as optic cavitation. Elementary particles such as protons, neutrinos, and photons can also be used to break down a liquid medium to produce cavitation, in what is often known as particle cavitation [5]. Both optic and particle cavitation are the consequence of a local deposition of energy [6]. They are frequently employed in laboratory environments for fundamental studies on cavitation, since single cavities or specially required cavities can be generated in this

* Corresponding author.
E-mail address: ying.zheng@uwo.ca (Y. Zheng).

way [7]. Acoustic and hydrodynamic cavitation, on the other hand, were first studied and widely applied in both academia and industry, due to the ease of operating and generating the required intensities for cavitation conditions. Like the discovery of cavitation in hydraulic systems, acoustic cavitation came to researchers' attention due to incidents involving an underwater sound projector in the 1920s, when an unexpectedly shorter distance of sound transmission and the frequent destruction of sound transducers were observed [8]. Ultrasound with a frequency ranging from 20 kHz to 1 MHz propagates through a liquid medium, generating mechanical vibration and negative local pressures, which result in acoustic cavitation. The chemical effects of acoustic cavitation were quickly recognized by chemists. This research has become so prevalent that the entire field of "sonochemistry" is dedicated to describing research on understanding the effect of ultrasound in forming acoustic cavitation in liquids. However, the short wavelength of ultrasound severely limits its transmission distance. This inherent aspect of ultrasound results in the critical drawback of low scalability, which hinders the application of acoustic cavitation in large-scale commercial operations.

Hydrodynamic cavitation can be generated via pressure fluctuations induced by varying the flow velocities of a liquid medium. It is achieved either by the passage of liquid through a constriction in a system, such as an orifice or venturi, or by the rotation of an object within a liquid. Hydrodynamic cavitation bubbles have patterns of behavior similar to those of acoustic cavitation bubbles [5]. Based on a numerical simulation, Moholkar et al. [9] suggested that the intensity of sound waves in the case of acoustic cavitation and the recovery pressure downstream in the case of hydrodynamic cavitation are similar to each other; the frequency of the ultrasound and the pressure recovery rate are analogous to each other as well. However, acoustic cavitation tends to generate highly intense cavity collapse, while hydrodynamic cavitation can create a large quantity of cavities with relatively low intensity [10]. With similar cavitational outcomes to acoustic cavitation, hydrodynamic cavitation features key advantages, including easy scale-up, low capital cost, and high efficiency. Therefore, hydrodynamic cavitation is a promising alternative to acoustic cavitation [5] and has been applied in various commercial settings for process intensification [11]. There has been an exponential increase in research efforts in hydrodynamic cavitation since 2000 (Fig. 1). Among these publications, five different categories can be observed: theoretical/experimental studies, the utilization/production of biomass, wastewater treatment, process intensification/reaction optimization, and medical/nanotechnology.

There are many excellent review articles that cover the hydrodynamics of cavitation bubbles, as well as the application of cavitation in wastewater treatment, biochemical engineering, renewable energy, the food industry, and so forth [3]. In addition to presenting recent research developments in hydrodynamic cavitation, the present article reviews hydrodynamic cavitation reactors (HCRs; including commercial cavitating reactors), radical-induced chemical processes, and scaled-up processes for the first time.

2. Mechanism of hydrodynamic cavitation

Cavitation bubbles (i.e., cavities) generally appear as the local pressure decreases to below the liquid vapor pressure. Bernoulli's principle provides a guideline for achieving pressure reduction in a flow system. Variations in the liquid velocity and pressure distribution in a flow field are described in Eq. (1). A constriction is frequently used in the passage of a fluid to increase the fluid velocity, which in turn induces a pressure reduction at the constriction. Venturi tubes and spray nozzles are common examples.

$$p_1 + \frac{1}{2}\rho v_1^2 = p_2 + \frac{1}{2}\rho v_2^2 \tag{1}$$

where ρ is the density of the fluid, p_1 and p_2 denote the pressures at two points (usually, upstream and downstream, respectively) in a flowing system, and v_1 and v_2 are their corresponding fluid velocities, as shown in Fig. 2. The liquid velocity in the tube increases at the expense of pressure. At the throat of the system, the liquid reaches its highest velocity (v_2) where the pressure (p_2) drops to its lowest value.

Vapor bubbles are assumed to form when the local pressure drops below the vapor pressure of the liquid at the given temperature [12]. If p_2 becomes lower than the vapor pressure of the liquid, vapor bubbles may appear. At a point downstream of the constriction, a sudden pressure recovery occurs simultaneously with the collapse of the bubbles, where a significant amount of energy is released [1]. The lower the throat pressure, the more severe the cavitation, and the more intense the energy discharged. It is crucial to predict the inception of cavitation since it not only plays an important role in the explanation of cavitation physics but also helps in studying the flow patterns during the hydrodynamic cavitation process and in designing cavitation devices.

2.1. Inception of cavitation

Cavitation inception defines the initiation of a cavitation phenomenon. Either for avoiding the formation of cavitation or for making good use of cavitation, cavitation inception is a key parameter in predicting the hydrodynamics of a liquid flow. It is a complex subject that depends on a wide range of factors, including seeding nuclei, fluid velocity and physical properties, and system pressure. Although extensive research efforts have been made, cavitation inception is still far from being completely understood at the present time. Thoma [13] was the first to suggest an index of cavitation (σ) to describe cavitation:
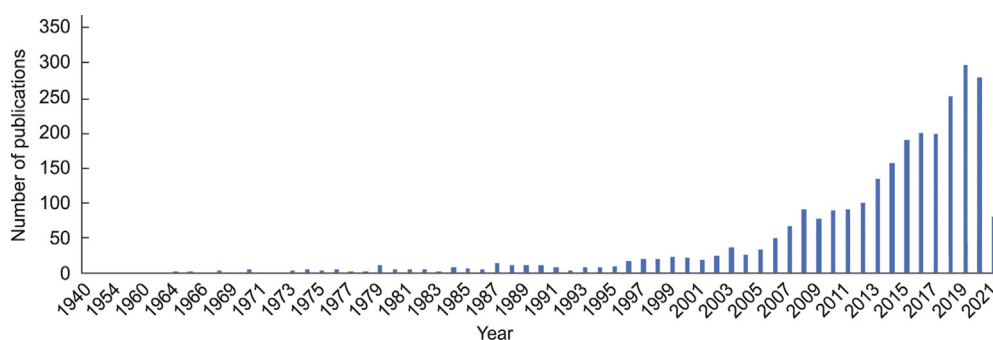

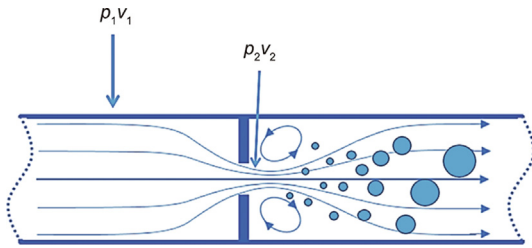Fig. 1. Publications on hydrodynamic cavitation from 1940 to 2021.

Fig. 2. A graphic illustration of hydrodynamic cavitation.

$$\sigma = \frac{p_s - p_v}{\Delta p} \qquad (2)$$

where p_s is the suction pressure of the pump, p_v is the vapor pressure of the liquid corresponding to its temperature, and Δp is the pressure rise obtained from suction to discharge at the best efficiency point of the pump.

This parameter was first suggested for use with pumps but had the disadvantage that variations in parameters occur from pump to pump. In an investigation of an open liquid flowing over a submerged object, Plesset [14] proposed a cavitation parameter, K, to qualitatively correlate flow patterns. When K is small, the cavitating flow pattern can be established.

$$K = \frac{p_o - p_v}{\frac{1}{2}\rho\, v_o^2} \qquad (3)$$

where p_o is the static pressure, and v_o is the uniform flow velocity at a distance from the body.

The cavitation parameter, which is now known as "cavitation number" in the current literature, is an important parameter in characterizing cavitation flow. In an open water system, every flow has a cavitation number, and increasing the fluid velocity results in a decrease in the cavitation number. Cavitation inception is characterized by a cavitation cloud. According to Eq. (3), for a specific liquid, both static pressure and liquid velocity are parameters that influence the cavitation number. This dimensionless number has also been applied to closed systems such as orifices and venturi, where the pressures and liquid velocities need to be specified (a detailed discussion is provided below). A lower value of cavitation number results in a higher probability of cavitation occurrence or in an increase in the magnitude of cavitation [15]. Bagal and Gogate [16] claimed that cavitation occurs when the cavitation number is dropped to about 1, and that the best cavitation performance is obtained at a cavitation number ranging from 0.1 to 1.0.

Cavitation inception is a complex phenomenon and is associated with many characteristics, among which cavitation nuclei is the most important. Cavitation nuclei can be considered as weak spots in a liquid, which may contain a mixture of vapor and non-condensable gases. They facilitate the development of cavitation by reducing the minimum required tensile strength of the liquid. (A detailed discussion is provided in the following section.) The dynamics of bubbles are complex and are associated with a variety of factors, including surface tension, viscous effects, and non-condensable content.

Not surprisingly, it is impossible for cavitation number to account for all the complexities; thus, it alone is insufficient to determine the conditions for cavitation inception, because it is highly dependent on other physical properties. Šarc et al. [12] observed that cavitation inception can be affected by several factors, such as constriction geometry, medium temperature, and the density and sizes of cavitation nuclei. Yan and Thorpe [17] reported a similar observation—namely, that the cavitation number is highly associated with the geometry. They further stated that the cavitation inception number varies between 1.7 and 2.4 for an orifice-to-pipe diameter ratio ranging from 0.4 to 0.8. Cioncolini et al. [18] suggested that micro-orifices could have much a lower cavitation number at the inception. Table 1 [17–21] summarizes the cavitation inception numbers reported in the literature. It can be seen that the cavitation number marking the inception of cavitation can greatly vary from well below 1 to more than 3, depending on the operational conditions, geometry, nuclei, and so forth. Thus far, accurate prediction of cavitation inception is still a difficult task. Current understanding of the inception of cavitation still heavily relies on experimental observation.

Eq. (3) was first developed to determine a cavitation number based on the tests performed in an open water system, which primarily characterized the cavitating flow occurring in open systems, such as hydrofoils. This dimensionless parameter has also been widely applied to orifices or venturis of closed systems where (partial) choking of the flow is expected to occur. Confusion arose when Eq. (3) was applied to a closed system. On the one hand, cavitation number itself is insufficient to illustrate the detailed situation inside a hydraulic system, as it is highly dependent on the system's own properties, such as operating conditions, designed structures, and so forth. On the other hand, there are a few pressures and velocities at various locations that are relevant to the constriction in an orifice/venturis system. Šarc et al. [12] conducted a test and calculated the cavitation number using various combinations of the pressure and velocities. For the same trials, by applying the pressures and velocities measured at different locations of the

Table 1
Cavitation numbers for the inception of cavitation.

Parameters used	Cavitating device	Device details	Cavitation number	Ref.
Downstream pressure, orifice velocity	Multiple orifice	Orifice diameter of 3 mm, pipe diameter of 3.78 cm	Cavitation inception number varies between 1.7 and 2.4 for orifice to pipe diameter ratio from 0.4 to 0.8	[17]
Downstream pressure, orifice velocity	Multiple orifice	Orifices with diameter of 0.15 and 0.30 mm and thickness of 1.04, 1.06, and 1.93 mm	Cavitation inception number varies around 0.3, 0.7, and 1.1 for three orifices	[18]
Outlet static pressure, inlet flow velocity	Modeling	—	Cavitation inception number varies from 0.36 to 1.00	[19]
Outlet static pressure, throat velocity	Venturi tube	Throat diameter of 10 mm, convergent angle of 45°, divergent angle of 12°	Development tendency of cavity occurs at cavitation number around 0.51, cavitation inception number of 0.99, cavitation number independent of inlet pressures	[20]
Reference pressure, reference velocity	Microfluidic devices with rough surfaces	Hydraulic diameters of 75.0, 66.6, and 50.0 μm and length of 2 mm, roughness of 5 μm	Different upstream pressures up to 900 psi (6.2 MPa) are applied, cavitation number ranges between 2.025 and 0.720, cavitation inception ranges between 0.925 and 3.266	[21]

testing system, they found that the value of the cavitation number varied roughly between 1.2 and 168.0. In the literature, inconsistences have also been observed. Some research groups have directly applied the downstream pressure and velocity (that is at a distance from the cavitation spot) to estimate the cavitation number. Instead of the downstream pressure and velocity, other research groups have employed the pressure and velocity at the constriction in order to take the choking of the flow into account. Ambient pressure, upstream pressure, and velocity have also been reported as being used in the determination of cavitation number. Table 2 [22–30] provides a summary of cavitation numbers obtained by employing different pressures and velocities. The selection of pressure and velocity can greatly influence the numerical estimation of the cavitation number and further affects the determination of cavitation inception. Thus, the definition of cavitation number needs to be refined when it is applied to a closed system. Further research on the theoretical understanding and characterization of cavitation in closed systems, including reactors, is in high demand.

2.2. Cavitation nuclei

Liquid vaporization tends to occur at free surfaces, such as gas bubbles and solid particles, which are known to be the source of cavitation formation and are called "cavitation nuclei." Nucleation is the accumulation of gas molecules to form micron-sized bubbles. For a pure liquid that is free of preexisting nuclei, its nucleation can only be realized through separation of the liquid molecules, at which point new phases are created. This is termed homogeneous nucleation. Using pure deionized water at 20 °C as an example, cavitation cannot be initiated until the local tensile strength is as low as −60 MPa [31]. However, cavitation is well observed in open water (seawater) and in tap water due to the presence of gas bubbles. The tensile strength of such waters is typically well below 1 bar (0.1 MPa) [32]. This finding indicated that nuclei play a key role in the formation of cavitation.

When inhomogeneities preexist in liquid to serve as nuclei, heterogeneous nucleation takes place. In practice, heterogeneous nucleation most likely dominates the formation of cavitation. Two distinct types of nuclei have been studied in the literature: free-stream nuclei, which freely float in liquid media; and surface nuclei, which are attached to a surface or a wall (Fig. 3) [33]. Surface nuclei are also known as Harvey nuclei, and can only be formed when two criteria are met: ① The surface to which the nuclei are attached should be hydrophobic. Nuclei on hydrophilic surfaces are unstable unless they are covered by organic skins. ② Gaps with conical shapes acting as an active site for gas nucleation should exist [33]. Harvey nuclei frequently exist in porous particles and are attached to jagged particles when particles are floated in liquid. When the pressure falls below the threshold pressure, rapid growth of surface nuclei is observed. It is said that the onset of cavitation is mainly associated with free-stream nuclei, and surface nuclei only play a minor role [33].

Free-stream nuclei are non-condensable gas bubbles entrapped in liquid. Due to the concentration gradient of the gaseous components in the liquid media, mass is expected to diffuse from the bubble surface to the bulk liquid. The equilibrium of a gas bubble in liquid is limited by the quasi-static stable balance of the far-field pressure and the Laplace pressure with the gas and vapor pressures inside the bubble.

$$p_c - p_v = \frac{-2}{3\sqrt{3}} \sqrt{\frac{\left(\frac{4S}{d}\right)^3}{p_\infty - p_v + \frac{4S}{d}}} \tag{4}$$

Table 2
Determination of cavitation number using various pressures and velocities.

Parameters used	Cavitating device	Device details	Findings	Ref.
Downstream pressure, orifice velocity	Multiple orifice	Orifices with diameter varies from 2 to 22 mm, pipe diameter of 26.64 mm	Cavitation number ranges from 0.09 to 0.99, optimum cavitation number is 0.13	[22]
Downstream pressure, orifice velocity	Venturi tube	Orifice diameter of 2 mm, outlet angle of 6.4°	Cavitation number ranges from 0.09 to 0.45, with fluid velocity from 46.62 to 20.78 m·s^{-1}	[23]
Downstream pressure, orifice velocity	Venturi tube	Throat diameter of 1.2 mm, tube diameter of 3.6 mm	Pressure ranges from 0.1 to 0.6 MPa, with peak cavitation number of 0.4	[24]
Downstream pressure, orifice velocity	Multiple orifice and venturi tube	Orifices with diameter of 2 and 3 mm, throat diameter of 2 mm	Cavitation number ranges from 0.11 to 0.57 with operating pressure from 5 to 15 bar, optimum cavitation number in the range of 0.17–0.20	[25]
Downstream pressure, jet velocity	Re-entrant jet	—	Cavitation number varies from 0.7 to 1.2	[26]
Ambient pressure, average orifice velocity	Sharp-edged orifices	Orifice diameter of 2 mm, pressure between 0.02 and 1.50 MPa	Cavitation number obtained from 0.4 to 2.0	[27]
Upstream pressure, flow velocity	Two-dimensional hydrofoil with circular leading edge	50.0 mm wide, 107.9 mm long, and 16.0 mm thick symmetric hydrofoil with circular leading edge and parallel walls	Cavitation number ranges from 2.0 to 2.5	[28]
Inlet pressure, impeller velocity	Impeller	—	Cavitation number ranges from 0.0138 to 0.2112	[29]
Characteristic pressure, characteristic velocity	NACA 16-020 foil	—	Cavitation number ranges between 0.69 and 2.02 for water quality tests, 0.40–0.96 for velocity scale tests	[30]

NACA: National Advisory Committee for Aeronautics.
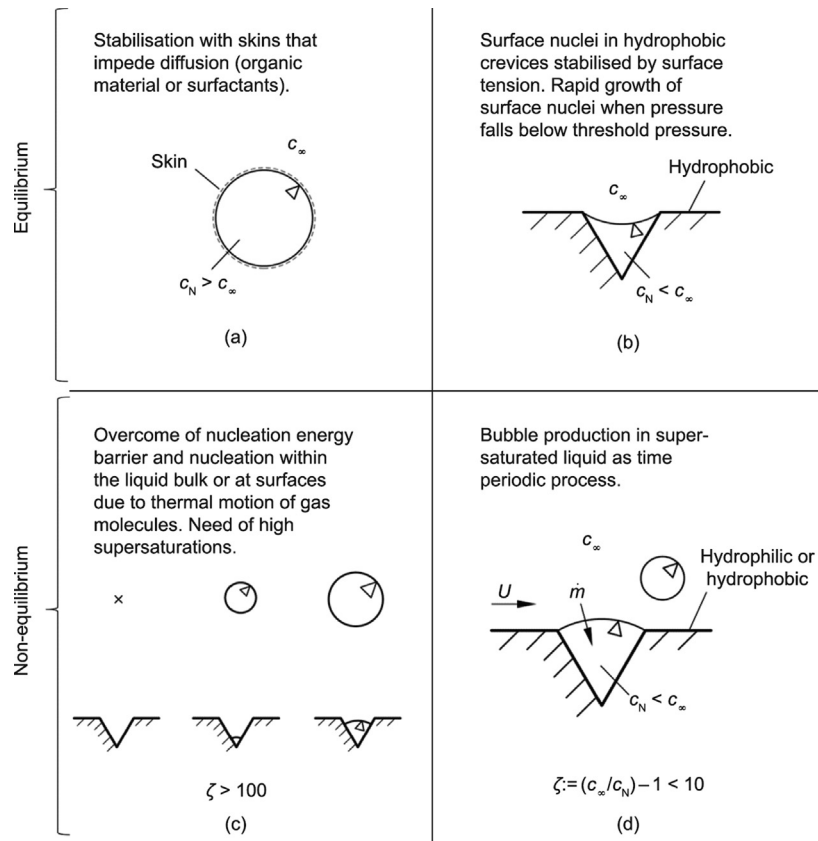1 bar = 10^5 Pa.

Fig. 3. Graphical illustration of two different types of nuclei. (a) Free bubbles; (b) Harvey nuclei; (c) classical nucleation; (d) diffusion-driven nucleation. c_N: local saturation concentration at the surface nucleus; c_∞: the concentration of gas in the liquid; ζ: the supersaturation of the liquid; $\dot{m}$: the mass flux of gas that diffuses into the surface nucleus; U: typical velocity. Reproduced from Ref. [33].

where S is the surface tension and d is a function of bubble diameter; p_c and p_∞ are the size-dependent critical pressure and ambient pressure, respectively [34]. This equation indicates that gas bubbles become unstable when the pressure drops below the critical pressure p_c. Although microbubbles are likely to be thermodynamically unstable due to gas diffusion, it is a fact that microbubble nuclei and their long-term stability are frequently observed in both natural and laboratory environments. Thus, the nuclei must be stabilized one way or another [35]. Khoo et al. [34] have claimed that the critical pressure, p_c, is well below vapor pressure when microbubbles are smaller than a 100 µm diameter. When gas bubbles were reduced to a few microns, Khoo et al. [34] found that the required p_c was dropped to several atmospheres of tension, and they confirmed that microbubbles could stably exist in water. Hsiao and Chahine [36] applied a Reynolds-averaged Navier–Stokes (RANS) solver to simulate bubble nuclei populations and confirmed the important role of gas diffusion in the dynamics of microbubbles. The average bubble size almost doubles, from 60 to 100 µm, when gas diffusion is considered. By introducing free gas bubbles that serve as cavitation nuclei, Tandiono et al. [37] obtained intense cavitation events even before the liquid flow dropped below its vapor pressure. These phenomena were recorded using a high-speed camera. The imploding cavitation bubbles were triggered by free gas bubbles introduced into the liquid moving toward the constriction. The microbubbles observed were in the range of hundreds of microns.

Bubble nuclei concentrations and critical pressures have been observed to be inversely correlated with system pressure but to increase with an increase in the saturation level of the dissolved gas. Russell et al. [38] demonstrated that the population and size

distribution of nuclei are strongly associated with the pressure of the test section. Increasing pressure leads to a reduction in the number of bubble nuclei. A similar result was observed by Pascal et al. [39], who used acoustic measurement technology. When the system pressure was in a negative pressure range, it was observed that a reduction of pressure led to a decreased number density of large nuclei (nucleus radius (R) > 10 µm) and an increased number density of small nuclei ($R < 10$ µm) [40].

The effects of gas saturation were reported by Shah et al. [8], who claimed that increasing gas solubility promoted the number of cavitation nuclei and lowered the cavitation threshold. Similar results were obtained by Hemmingsen [41], who further stated that the impact on cavitational effects became less important when the gas solubility was very high. Venning et al. [42] confirmed the above statements by using a cavitation susceptibility meter (CSM) measurement. The nuclei size distributions were studied in an air–water system in cavitation tunnels under laboratory conditions. The researchers noticed that the quantity of bubble nuclei remarkably increased with the concentration of dissolved gas when the water was oversaturated. However, the impact was significantly weakened when the water was not saturated with dissolved gas. This result suggests that gaseous diffusion plays a role in microbubble population dynamics.

In contrast to the microbubbles discussed above, "nanobubbles" are bubbles with a diameter of less than 1 µm. As mentioned in the last section, a gas bubble is stabilized based on the pressure balance inside and outside of the bubble. The Epstein–Plesset theory predicts that the pressures can be balanced in a saturated liquid under very narrow circumstances so that nanobubbles are unlikely to survive for any significant amount of time under uncontrolled

circumstances. The lifetime of nanobubbles (radius < 1000 nm), as predicted by the Epstein–Plesset theory, is less than 0.02 s; thus, bubbles should dissolve and disappear quickly. The skin stabilization theory proposed by Fox and Herzfeld [35] provides a basis for the development of stabilized nanobubbles. The theory states that an organic skin (generated by a surfactant or other organic chemicals) covering a bubble surface terminates or slows down the gas diffusion between gas bubbles and liquid media, and thereby slows bubble collapse. An early direct observation of bulk nanobubbles (less than 1 μm) was reported by Johnson and Cooke [43]. Attention has been given to nanobubbles with the development of nanotechnology. A variety of techniques have been applied to generate stable nanobubbles, whose physical properties and concentrations have been carefully studied. By depressurizing pre-air-saturated deionized water, Calgaroto et al. [44] generated highly loaded nanobubbles that remained stable for 2 weeks. Etchepare et al. [45] used a centrifugal multiphase pump (CMP) and a cavitation zone to generate concentrated nanosized air bubbles in aqueous solutions. This work demonstrated the likelihood of highly stable nanobubbles being present in aqueous solutions. Aside from air, gases such as N_2, CH_4, and Ar have also been used to produce nanobubbles in water. Such bubbles are extremely dense, with a density as high as 10^{13} bubbles per milliliter, and long lived, lasting for up to 2 weeks [46]. Fig. 4 [46] shows a scanning electron micrograph of nanobubbles with an average size of 50 nm in an aqueous solution. Stable nanobubbles were also observed in organic solvents [47].

On the current market, there are commercially available devices that can generate stable nanobubbles. Azevedo et al. [48] reported that a high concentration of nanobubbles (6.4×10^8 bubbles per milliliter) was generated by the patented sparger CavTube, which creates nanobubbles via an abrupt contraction and expansion of a water-and-air mixture. Fig. 5 [48] shows an image of air nanobubbles in dilute methylene blue distilled water, recorded using an optical microscope with backlight and an objective magnification of 1000 times.

Nanobubbles have attracted a great deal of wide-ranging interest in the fields of science and technology. Flotation is widely used in the mining industry, and nanobubbles have been extensively studied in the separation of fine particles. Nanobubbles tend to attach to fine powders, resulting in particle aggregation and allowing fines to be recovered in the froth flotation process [49]. Nanobubbles also have numerous potential applications in the food industry, ranging from beverages and baked products to fro-
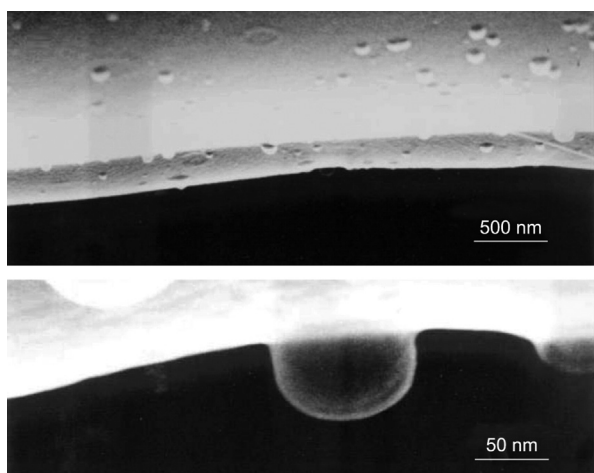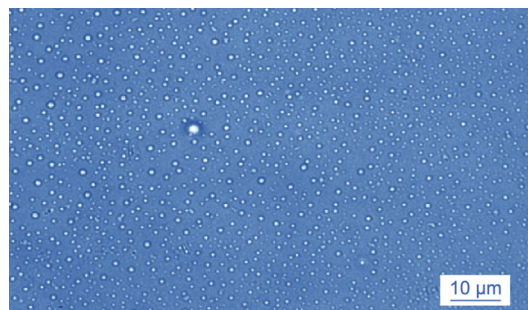

Fig. 5. An image of nanosized air bubbles in water. Reproduced from Ref. [48] with permission.

zen food [50]. For example, introducing nanobubbles to a food system can effectively enhance the freezing rate and reduce the total freezing time, since nanobubbles provide huge amounts of nuclei for the formation of ice crystals. The effective application of nanobubbles has also been studied in the agricultural sector. Michailidi et al. [51] reported that nanobubbles can enhance plant growth. Tomato plants were watered using tap water and water saturated with nanobubbles of air, oxygen gas, and nitrogen gas, respectively. The researchers found that the tomato weight increased by 25.5%, 32.7%, and 58% for air-, oxygen-, and nitrogen-enhanced nanobubble water, in comparison with tap water. In recent decades, nanobubbles have also been studied as an effective tool in biomedical applications [52]. Zhou et al. [53] reported a novel technique to synthesize stable protein-shelled nanobubbles for diagnostics and nuclei acid delivery. Nanobubbles ranging in size from 400 to 700 nm can enhance the loading capacity of oligonucleotides by up to 1.6×10^3 DNA molecules per nanobubble. Other potential applications of nanobubbles include wastewater treatment, water purification, and surface cleaning [51,54].

This documented evidence has confirmed that nanobubbles (either of air or of other types of gases) can survive in water and organic solutions for a significant period of time without an organic "skin"—phenomena that are difficult to interpret using either the Epstein–Plesset theory or that of Fox and Herzfeld. A number of explanations have been proposed. For example, gas saturation and interactions between highly concentrated nanobubbles have been considered. This explanation is limited to extremely high concentrations of gas bubbles [55]. The dynamic equilibrium model [56] explains the stability of nanobubbles attached on solid particles but becomes invalid for systems that contain no solid particles. To date, the explanations that have been proposed may be rational only for individual situations. A widely acceptable theory has not been identified for the interpretation and prediction of the long-term stability of nanobubbles under different conditions [57].

2.3. Cavitation-influencing factors

2.3.1. Temperature

Fluid temperature is a determining factor that influences nuclei formation and cavitation events in many cases, including chemical reactions, hot fluid injection, and cryogenic cavitation. Theoretically, temperature functions distinctly in a cavitating flow. On the one hand, increasing the temperature at the same ambient pressure promotes liquid vaporization, resulting in a greater aptitude to cavitate; on the other hand, it demotes the cavitation phenomena because of reduced vapor pressures within the gas bubbles. The latent heat of evaporation of the liquid lowers the temperature around the bubbles and therefore decreases the vapor

Fig. 4. Nitrogen nanobubbles in an aqueous solution. Reproduced from Ref. [46] with permission.

pressure within the bubbles. It is worth noting that increasing the temperature generally reduces gas solubility in a liquid medium, so the number of cavitation nuclei, which is the crucial factor in cavitation initiation, is reduced. This leads to a higher threshold for cavitation initiation. Extensive research on the effects of temperature on cavitation were performed in the last century, and it has been widely accepted that increasing the temperature increases the cavitation number, delays cavitation inception, and lowers cavitation intensity [58]. Recent studies have confirmed the negative impact of the thermal effect on cavitation nuclei. Niemczewski [59] observed that the cavitation intensity increased with decreasing temperature in water that was chemically deoxidized and weakened as the temperature rises. Similar results were reported by Torre et al. [60], who claimed that thermal effects are inversely associated with cavitation intensity. This conclusion was derived from the degradation performance being worsened with temperature. Li et al. [61] used dissolved oxygen and nitrogen as cavitation nuclei to study the tensile strength of water and concluded that a higher gas concentration results in a higher cavitation probability. The fact that the solubility of both oxygen and nitrogen decreases significantly at elevated temperatures is responsible for a lower cavitation probability. De Giorgi et al. [62] observed that temperature has a mixed effect. In the 293–333 K range, increasing the temperature led to a higher cavitation number; however, beyond this range, further increasing the temperature to 348 K resulted in a decrease in the cavitation number, provoking the start of cavitation.

2.3.2. Pressure

Pressure is an important variable that can influence the inception of cavitation. Since vapor pressure and downstream pressure are frequently used to calculate the cavitation number of a flow, investigating the inlet pressure may be worthwhile. Despite its simplicity in measurement and in control, attention was not given to the influence of inlet pressure on cavitation until the last two decades. Soyama [24] studied the influence of upstream and downstream pressures on cavitation intensity using a venturi tube with water as the liquid medium. He observed that, when the downstream pressure was kept constant, the cavitation region increased monotonously with increasing upstream pressure, as visualized in Fig. 6 [24]. When the upstream pressure was kept constant, cavitation developed, and the intensity increased quickly with decreasing downstream pressure.

Joshi and Gogate [63] demonstrated that dichlorvos hydrodynamic cavitation degraded faster when the inlet pressure was increased. Their results indicated that increasing the inlet pressure led to an increase in both the downstream pressure and the rate of pressure recovery. Kumar and Pandit [64] reported severe turbulent downstream flow and violent cavity collapse at higher inlet pressures, which they attributed to the large pressure drop across the orifice induced by high inlet pressure. When studying a regulating valve, Liu et al. [65] found that both the cavitation zone and the intensity increased with inlet pressure. The enhanced cavitation phenomena caused by higher inlet pressure have been further investigated by means of numerical simulation [66]. If the inlet pressure fluctuates following a sine wave, the cavitation process and flow structure fluctuate accordingly. The amplitude and frequency of the fluctuation have a great influence on the cavitation. There is an optimal frequency suppressing the occurrence of cavitation. However, inlet pressure corresponds to system pressure. Increased system pressure can have a negative effect on the generation and intensity of cavitation.

2.3.3. Physical properties of a liquid medium

The physical properties of a liquid medium include volatility and viscosity. There have been contradictory reports on the effects of the volatility of a liquid medium. Taşdemir et al. [67] observed that volatile solvents can be efficiently removed from wastewater
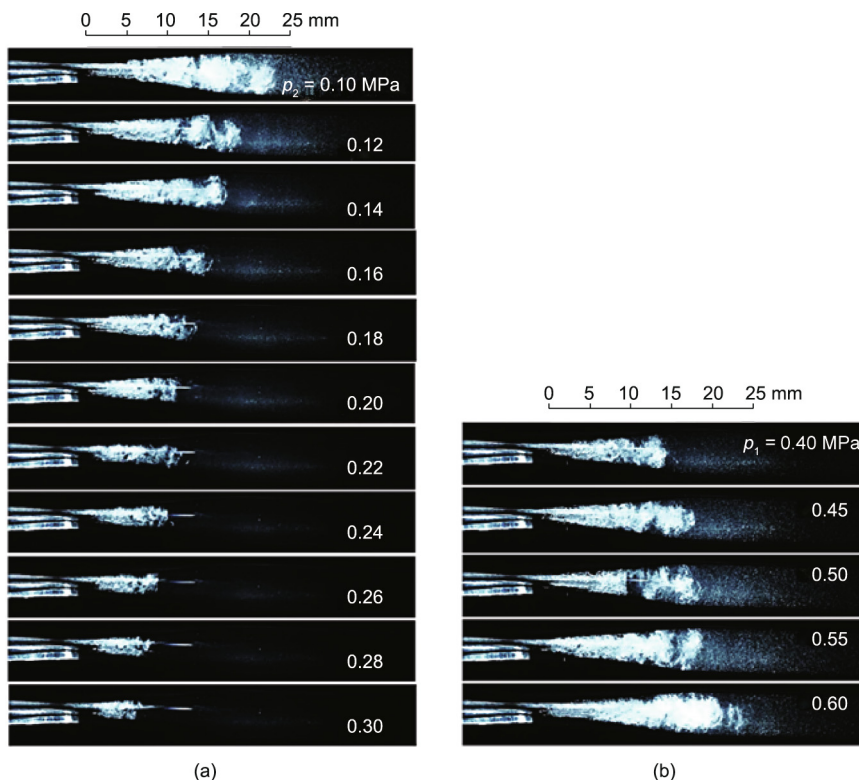

Fig. 6. Cavitation varies with upstream and downstream pressures. Aspects changing with (a) downstream pressure p_2 (p_1 = 0.6 MPa) and (b) upstream pressure p_1 (p_2 = 0.1 MPa). Reproduced from Ref. [24].

(98.4%) by an HCR, even in the absence of aeration. The evaporated vapor in a liquid medium usually acts as nuclei to enhance cavitation [34]. On the other hand, easy evaporation of highly volatile liquid may result in difficulty in preventing the vapor from escaping the liquid phase, so that a smaller number of cavities can be maintained in the liquid phase [68]. Bebchuk et al. [69] studied the metal erosion caused by the impact of cavitation and concluded that cavitation could be promoted only when the liquid vapor pressure ranged from 35 to 80 mmHg (4.66–10.66 kPa) for liquids such as water and ethanol. This finding suggests that an optimal vapor pressure—and thus an optimal volatility of a liquid—exists for promoting cavitation.

Liquid viscosity can influence the formation and collapse of cavitation bubbles. Although liquids with higher viscosity, such as oils or monomers, are common in various industrial applications, research on the effects of viscosity on the cavitation process remains scarce, especially in terms of experimental studies on cavitation. Surprisingly, almost all relevant work has only been conducted at the theoretical level [70]. These results suggest that a liquid must overcome its internal forces to produce cavities, so that any increase in these forces will lead to an increase in the energy required to initiate cavitation. Experimental observations have confirmed this suggestion [71,72]. A more viscous liquid requires more energy to entrap air bubbles as nuclei; therefore, high viscosity tends to retard the evolutionary process of cavitation bubbles. The effects exerted by liquid viscosity on cavitation are not as significant as those exerted by temperature and pressure. Arndt [73] stated that the variation in cavity collapse pressure is not significant with increasing viscosity. Later, Nazari-Mahroo et al. [74] confirmed that the bulk viscosity has a minor effect on the cavitation dynamics, based on the study of a single cavitation bubble. However, the relationship between viscosity and cavitation intensity is still unclear due to the lack of experimental studies.

3. Cavitation-induced reaction enhancement

Bubble collapse in the process of cavitation releases a large amount of energy, accompanied by extremely high local temperatures and pressures [75]. The recorded spectrum of sonoluminescence suggests a temperature of 5000 K due to bubble collapse [76]. Qin and Alehossein [77] suggested that the maximum temperature could be dramatically increased with the size of bubbles. These extreme local conditions also generate chemically active free radicals (OH·, H·), ultraviolet (UV) radiation, strong local turbulence, microjets, and shock waves of a few thousand atmospheric pressures—special features that are anticipated to significantly enhance mass and heat transfer, as well as chemical reactions. Hydrodynamic cavitation has been applied to various chemical and biochemical processes and environmental applications.

3.1. Cavitation-enhanced heat transfer

It is well known that the collapsing bubbles in hydrodynamic cavitation generate hot spots and violent turbulence. These phenomena have encouraged researchers to explore the applications of cavitating flow by directly harvesting the thermal energy and/or enhancing the rate of heat transfer. Russian scientists have made efforts to develop hydraulic heat generators to directly collect the heat generated by hydrodynamic cavitation. Zaporozhets et al. [78] reported experimental results on the vortex and cavitation nonuniform flows occurring in a hydraulic heat generator and demonstrated that the heating efficiency decreases with increasing liquid temperature due to the growing saturation vapor pressure. A cavitation heat generator model was later tested by Little [79], who reported the achievement of 80% efficiency. Pyun et al. [80]

continued the study of cavitation-based heaters and reported a cavitation heat generator in which cavitation bubbles were produced by rotating a disk at high velocity. The generation of heat energy and thermal efficiency were evaluated against several variables, including inlet pressure, rotational velocity, and inlet velocity. The researchers reported a heat efficiency of up to 94%. Later, the same research group applied a similar device to disinfect water [81]. Their results showed that 48.15 MJ·h^{-1} of heat could be generated, and a thermal efficiency of 82.18% was achieved. The generated heat was directly used to heat water up to 61.9 °C so that *Escherichia coli* (*E. coli*) in the water was successfully destroyed.

Aside from making use of the heat generated by cavitation bubbles, a considerable amount of research has been done to understand the role of collapsing bubbles in enhancing the rate of heat transfer [82]. Special attention has been given to the effects of acoustic cavitation on heat transfer. Relatively few studies have focused on hydrodynamic cavitation-enhanced heat transfer. Given the limited documentation, the effects of hydrodynamic cavitation on heat transfer mechanisms have primarily been studied in microchannel systems. It has been found that the turbulence flow and microjets caused by cavitation play a key role in enhancing the rate of heat transfer, both within the system and from the wall to the system. Schneider et al. [83] experimentally studied the forced convection heat transfer induced by hydrodynamic cavitation in silicon channels, with deionized water as the liquid medium. They concluded that convective heat transfer was the dominant heat transfer mechanism. The intensity of cavitation is a positive factor in influencing the rate of heat transfer. The maximum heat transfer coefficient has been observed to increase by 67% due to the presence of the cavitation phenomenon. As deionized water was replaced by refrigerant fluid R-123, an increase in the rate of heat transfer of as high as 84% was achieved [84,85]. Cavitation-promoted heat transfer was further observed by another research using R-134a refrigerant fluid as the flow medium [86]. It was demonstrated that a heat transfer coefficient as high as 100 kW·(m^2·K)$^{-1}$ was achieved as the micro-orifice-induced hydrodynamic cavitation was presented in the proposed heat exchanger. This result doubled the highest value recorded in previously published studies [87]. Although most research in the literature has employed narrow orifices to induce hydrodynamic cavitation, some studies reported using a converging–diverging nozzle to induce hydrodynamic cavitation. Again, with R-134a refrigerant fluid as the flow medium, a heat transfer coefficient of up to 285 kW·(m^2·K)$^{-1}$ was observed in the proposed system [88].

In addition to experimental investigations, numerical studies such as computational fluid dynamics (CFD) have been carried out to understand the behavior of cavitation bubble collapse and its effect on heat transfer. Applying the volume of fluid (VOF) model and FLUENT commercial software, Liu et al. [89] studied the dynamic behavior of the cavitation bubble profile while considering wall effects in a microchannel system. Wall effects can be significant in a microchannel system due to the small scale. The simulated results indicated that heat transfer can be either enhanced or decreased depending on the energy of the generated microjets and the position of the cavitation bubbles with respect to the wall of the microchannel. An optimum initial bubble radius was identified for maximum heat transfer enhancement. To maximize the effects of cavitation on heat transfer, it is preferable for the bubbles to be positioned in the center between two parallel walls. The same research group recently proposed a three-dimensional (3D) numerical model to predict the interaction between two cavitating bubbles in a heated tube and its effect on heat transfer [90]. They confirmed that the microjets generated during bubble collapse play a key role in enhancing heat transfer.

3.2. Cavitation-enhanced mass transfer

As mentioned in the Section 2.1 of inception of cavitation, many physical and chemical effects are generated along with cavitation, and the mechanical effects produced during the process will reduce the resistance to mass transfer, as cavitational effects enhance the contact between gases and liquids by increasing the interfacial area. Cavitation also results in the generation of local turbulence and liquid micro-circulation within the medium, enhancing transport process rates [91–93]. To determine how hydrodynamic cavitation improves mass transport, many experiments have been done and several common evaluation standards have been used, including reaction rates, process yield, and local mass transfer coefficient.

Bubbles will be generated when the orifice pressure is reduced to a point lower than the liquid vapor pressure, and the mass transport is enhanced by these bubbles. The presence of microbubbles not only extends the surface area of interaction significantly but also creates a concentration gradient within mixed liquids and therefore maximizes the process output. Plesset and Prosperetti [94] stated that mass diffusion mostly takes place at the bubble–liquid interface, and it plays an important role in the behavior of gas bubbles, as the behavior can eventually determine the existence or absence of bubbles in a liquid. As for the bubble itself, mass diffusion and the radius of the bubble are related due to the following effects:

- **Concentration effect.** When a bubble expands, the concentration of the gas trapped within the bubble decreases and gas diffuses into the bubble; likewise, when a bubble shrinks, the concentration of the gas trapped inside increases, and the gas diffuses from the interior of the bubble.
- **Shell effect.** Since the rate of diffusion of a gas to a liquid is directly proportional to the concentration gradient of the dissolved gas, as the bubble contracts, the gas concentration outside the bubble wall decreases; therefore, the rate of gas diffusion away from the bubble is greater than equilibrium. Similarly, when a bubble expands, the gas content near the bubble wall is increased, and the diffusion rate toward the inside is greater than normal. Such convection has the net effect of improving the mass diffusion.

Cavitation bubble behavior has two main aspects: The first aspect is the oscillation amplitude of the bubble, which is mirrored by the magnitude of the resulting cavity collapse pressure. The second is the duration of the bubble, which is expressed in the distance traveled and thus the expansion of the cavitational impact zone from its source. Those two aspects are both highly related to the mass transfer that occurs during the hydrodynamic cavitation process. Moreover, Peng et al. [95] found that, due to the lowered pressure within the bubble, water vaporization occurs on the bubble wall during the expansion process. On the other hand, in the course of bubble collapse, the vapor may condense back into the liquid phase and be released out of the bubble. Due to the unbalanced concentration within and outside the bubble, the amount of non-condensable gases also varies because of mass transfer.

A great deal of research has been done to demonstrate the effectiveness of cavitation on improving the mass diffusion processes. Karamah et al. [96] used both acoustic and hydrodynamic cavitation to enhance the ozone mass transfer coefficient, which is a mathematical model proposed by Zhang et al. [97] and applied classic unsteady state methods. They found that the coefficient for hydrodynamic cavitation was around 1.6 times higher due to the increase in the mass transfer area as a result of the formation of bubbles; also, the enhancement obtained from mechanical effects was lower than that from chemical effects. Kelkar et al. [98] found that hydrodynamic cavitation was an efficient way (> 90% conversion) to intensify the esterification of acids for the

synthesis of biodiesel at ambient temperature and pressure. Milly et al. [99] used an HCR to improve the mass transfer from bulk fluid to the surface and proved successful in increasing the mass transfer of transparent fluid to the UV irradiated surface. Chuah et al. [100] also showed that the high turbulence generated by hydrodynamic cavitation was effective in reducing the mass transfer resistance by increasing the interfacial area. Braeutigam et al. [101] and Franke et al. [102] investigated the effectiveness of a combination of hydrodynamic and acoustic cavitation for the treatment of water and found that the combined technology had a synergetic effect. Arrojo et al. [103] stated that hydrodynamic cavitation serves as a very low-frequency ultrasonic reactor, creating large bubbles, a large pressure pulse, and OH radicals.

3.3. Physical effects

The mechanical effects of cavitation also enhance reactions in a gas–liquid system. The extreme temperature, pressure, and turbulence generated from the collision of cavitation bubbles leads to a significant structural and mechanical change. Furthermore, mass transfer not only exists between gas bubbles and the liquid boundary surface; it also happens at the interface between two or more liquid mediums. As millions of microscopic bubbles can be produced during the cavitation process, they generate powerful shockwaves that can destruct materials when the bubbles collapse. Therefore, Gogate [104] recommended hydrodynamic cavitation as a way to intensify the mass transfer between liquids, since the rate-determining step in many heterogeneous reactions is the mass transfer at the interface.

Inside a cavity, the gases and vapors are trapped adiabatically, creating extreme heat that increases the temperature of the surroundings directly and produces a localized hot spot upon collapse. Therefore, each cavity can be treated as a microreactor during the collapse phase, since both the temperature and pressure will reach the highest peak, and the entrapped organic molecules will thermally be decomposed into smaller molecules within this region. Although the temperature of this region is extremely high, the region itself is so tiny that the heat dissipates rapidly; therefore, the bulk of the liquid remains at a normal temperature.

At the same time, due to the oscillation of cavities and their subsequent collapse, high-shear microjets and turbulence are created in the interface region. The turbulence and mixing allow the particles to distribute uniformly and interact with each other sufficiently, which leads to the formation of fine emulsions. The available surface area is then greatly increased, enhancing the reaction rates. Therefore, the speed of reaction at the bubble–liquid interface is higher than that in the bulk liquid region. Furthermore, emulsions created by cavitation are typically more stable, and hardly any surfactant is required to maintain this stability. This is extremely helpful, especially in the field of phase transfer reactions [104].

3.4. Chemical effects

As mentioned in previous sections, extreme conditions can be produced during the vapor collapse process. In addition, free radicals (e.g., OH· and H·) are produced during the cavitation process due to the dissociation of water molecules trapped in the cavitating bubbles. These radicals are mixed with the bulk fluid and can either induce various chemical reactions or change the reaction mechanism. The main reactions involved in this process are given in Eqs. (5) and (6).

$$H_2O \rightarrow H\cdot + OH\cdot \tag{5}$$

$$OH\cdot + OH\cdot \rightarrow H_2O_2 \tag{6}$$
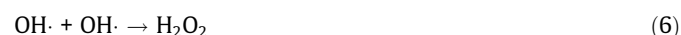
In recent decades, there has been growing interest in developing mathematical models to simulate cavitation phenomena and to predict free radical formation and the factors affecting radical formation [105–109]. Most of the documented modeling studies were generated based on acoustic-induced cavitation, due to its relatively easy generation of a controllable single bubble. Sochard et al. [110] proposed a model to correlate the generation of free radicals to bubble dynamics in an acoustic field, based on the assumption that dissociation reactions can occur at thermodynamic equilibrium at the maximum compression of bubbles. From the proposed models, they derived an optimal bulk liquid temperature for producing free radicals, which was verified by the experimental results obtained from aqueous oxidation reactions. Gireesan and Pandit [111] modeled the effects of carbon dioxide (CO_2) on cavitation via a diffusion-limited model coupled with chemical reactions. An increase in CO_2 concentration was found to inhibit the cavitation intensity. Both the collapse temperature and the yield of hydroxyl radicals were reduced as the CO_2 concentration increased in the gas bubbles. Fourest et al. [112] compared the single-bubble dynamics results from the classic Keller–Miksis model and finite-element simulations in a confined medium. The difference in amplitude and period was found to be 3% and 1%, respectively, for bubble dynamic, and the pressure transmitted was shown to have less than 1% variation for both methods.

3.5. Cavitation enhancement in various processes

3.5.1. Cavitation in wastewater treatment process

The hydroxyl radicals (OH·) produced in hydrodynamic cavitation process have been found to be the main reactive species involved in oxidation reactions, due to their huge reduction potential (2.7 eV). These radicals diffuse into the working fluid and participate in secondary oxidation reactions, which take place at the gas–liquid interface and in the bulk liquid. Due to their nonselective and extremely reactive nature, hydroxyl radicals can easily oxidize many susceptible organic molecules [113]. With this outstanding effect, the radicals become an effective tool for industrial wastewater treatment.

Badve et al. [114] used generated hydroxyl radicals to remove organic impurities in wastewater; they found that the addition of hydrogen peroxide enhanced the chemical oxygen demand (COD) removal, as additional hydroxyl radicals were available for the oxidation of wastewater. Similar results were reported by Saharan et al. [23], who indicated that the main mechanism for the destruction of pollutants is the attack of OH· radicals; they observed almost 100% decolorization and 60% reduction of total organic carbon (TOC). Joshi and Gogate [115] performed an experimental study on the intensification of industrial wastewater treatment using hydrodynamic cavitation combined with advanced oxidation; they found that hydrodynamic cavitation combined with Fenton and oxygen gas was the best approach. With the generation of hydroxyl radicals, this process removed 63% of the COD in wastewater within 180 min. Bandala and Rodriguez-Narvaez [116] also tested the effectiveness of hydrodynamic cavitation on the removal of water pollutants, using Congo Red and sulfamethoxazole as model contaminants. Based on their results, they suggested that the process is most likely thermally based rather than radically based, as organic pollutants could be degraded even when no hydroxyl radicals were produced.

The intensity of hydrodynamic cavitation can also be assessed by quantifying the production of OH· radicals. Arrojo et al. [117] used salicylic acid to evaluate hydrodynamic cavitation intensity, as the fluorescent reaction product of salicylic acid is specific for the determination of OH· radicals. Moreover, the analytical method they proposed, which was based on high-performance liquid chromatography, was demonstrated to be highly selective and sensi-

tive. The same method was used by Amin et al. [118], who confirmed that salicylic acid dosimetry is an effective tool to quantify hydroxyl radical generation in an HCR. However, Zupanc et al. [119] reported some anomalies detected during cavitation when using salicylic acid dosimetry to measure the production of hydroxyl radicals. They stated that cavitation appeared gentler, with less intense collapses, when a high concentration of salicylic acid was used, and the surface tension was found to be the most influential physical characteristic.

3.5.2. Hydrodynamic-cavitation-induced decomposition/degradation reactions

Aside from the generation of highly reactive species, extreme conditions produced by hydrodynamic cavitation can intensify chemical reactions. The tremendous implosion and shear forces produced by the collapse of vapor bubbles provide sufficient energy to break molecular bonds or thermally decompose organic pollutants, which can fulfil the need to degrade macromolecules and destroy microorganisms [120]. Rajoriya et al. [121] detected the degradation mechanism of rhodamine 6G, which was caused by the attack of OH· radicals. The researchers used hydrodynamic cavitation with the addition of tert-butanol and found that OH· radicals could be neutralized by tert-butanol to produce the less reactive tert-butanol radical, which limited the degradation rate. The results revealed that OH· radicals were the rate-limiting factor, and that they are mainly responsible for the degradation efficiency. Wang et al. [122] investigated the effects of combining hydrodynamic cavitation with hydrogen peroxide for the decomposition of rhodamine B in aqueous solution. The results showed that the degradation rate was greatly enhanced by the addition of hydrogen peroxide, due to its contribution to producing additional hydroxyl radicals. Wang et al. [123] studied the degradation level of tetracycline based on a combination of photocatalysis and hydrodynamic cavitation. They stated that the degradation of tetracycline was improved by about 1.5–3.7 times due to the increased generation of reactive hydroxyl radicals. Li et al. [124] investigated the removal of *Microcystis aeruginosa* using hydrodynamic cavitation; they observed a positive correlation between free radical concentration and algal reduction efficiency. Thus, algal reduction efficiency reached its highest level (over 95%) with an increase in hydroxyl radical concentration. Arrojo et al. [103] performed a parametrical study of disinfection with hydrodynamic cavitation and stated that disinfection was mainly caused by the mechanical disruption of bacteria, and that hydroxyl radicals only played a minor role.

3.5.3. Application of hydrodynamic cavitation in biodiesel production

Biodiesel is viewed as an excellent alternative to conventional petroleum-based fuel, as it can be simply derived from the transesterification reaction of vegetable and non-edible oil or animal fat with proper alcohol [125]. Therefore, biodiesel has received considerable attention in the bio-based economy; however, its production is generally limited by several factors, such as a long reaction/production time and a low mass transfer rate between alcohol and oil. In recent years, many researchers have used HCRs to produce biodiesel, since such reactors can produce biodiesel both efficiently and continuously [126].

Samani et al. [127] studied the enhancement of a rotor–stator type HCR on the production of biodiesel and were the first group to use safflower oil as the feed. They observed a 5.5% increase in the yield when the reaction time was extended from 30 to 60 s, and a decreased yield of 2.8% when the catalyst concentration was increased from 0.75% to 1.25%. The optimum yield of 88.62% occurred at a 60 s reaction time, a 1% catalyst concentration, and an alcohol-to-oil molar ratio of 8:1. Mohod et al. [128] demonstrated the effectiveness of a high-speed homogenizer for the

intensification of biodiesel production and compared the results when using waste versus fresh cooking oil as the feed stock. The optimum yield of biodiesel production was found to be 97% for waste cooking oil as the feed stock and 92.3% for fresh oil, under the optimum operating conditions of 120 min, a methanol-to-oil molar ratio of 12:1, 3 wt% of KOH as the catalyst, and 50 °C. A similar experiment was conducted by Innocenzi and Prisciandaro [129], who indicated that the introduction of an HCR decreased the energy consumption by about 40%, and that the use of waste cooking oil as the starting material further decreased the cost from 820–830 to 290–300 EUR·t^{-1}. Chuah et al. [130] performed a kinetic study on the conversion of waste cooking oil into biodiesel. They compared the results obtained for hydrodynamic cavitation and mechanical stirring. For cavitation, the rate constant was 7.7-fold higher and the feedstock per product was 4.6-fold lower in comparison with mechanical stirring. The activation energy for cavitation and stirring were 89.7 and 92.7 kJ·mol^{-1}, respectively. Overall, hydrodynamic cavitation is a viable approach to intensify biodiesel production with favorable economics.

3.5.4. Application of hydrodynamic cavitation in extraction/ emulsification

The mechanical effects of cavitation can enhance reactions occurring at the gas–liquid and liquid–liquid interface. The extreme temperature, pressure, and turbulence generated from the collapse of cavitation bubbles leads to significant structural and mechanical changes. Furthermore, as millions of oscillating bubbles with high interfacial area and a high intensity of micro-level turbulence are produced during the cavitation process, an HCR is very effective in eliminating the mass transfer resistance between phases. Therefore, HCRs have already been successfully applied to the extraction of bioactive compounds [131] and antioxidant pollutants [132].

Preece et al. [133] used hydrodynamic cavitation to extract protein from soybean cells; they found that only 1 pass at 100 MPa was sufficient to disrupt all soybean cells and achieve a maximum protein yield of 90%. Lee and Han [134] tested the ability of hydrodynamic cavitation to disrupt microalgae cells and perform lipid extraction. They obtained a maximum lipid yield of 45.5% from cells using 0.89% sulfuric acid with a cavitation number of 1.17 and a reaction time of 25.05 min. They also concluded that hydrodynamic cavitation was more energy efficient than autoclaving and ultrasonication in terms of specific energy input. Setyawan et al. [135] studied the extraction of algae oil from microalgae using hydrodynamic cavitation. They stated that the extraction process was feasible and that it was influenced by the amount of specific energy input, cavitation intensity, and temperature. The lowest extraction energy required was found to be 16.743 MJ·kg^{-1} lipid, and the optimum cavitation number and temperature were 0.126 and 42 °C, respectively.

At the same time, due to the oscillation of cavities and its subsequent collapse, high-shear microjet and turbulence are created in the interface region. The turbulence and mixing allow the particles to distribute uniformly and interact with each other sufficiently which leads to the formation of fine emulsions. Furthermore, the emulsion generated requires hardly any surfactant to maintain the stability and it is more stable compared to the conventional methods [136] since localized high temperature not only increases the reaction rate, but also the mass transfer rate due to the increase miscibility of reactants.

Carpenter et al. [25] studied the production of highly stable oil in a water emulsion using a hydrodynamic cavitation device. They obtained nano-emulsions with a droplet size of 87 nm that were found to be kinetically stable even under centrifugal and thermal stress conditions. The optimum operating cavitation number was 0.19 and the processing time was 90 min. Furthermore,

hydrodynamic cavitation was found to be 11 times more energy efficient than acoustic cavitation for the preparation of nano-emulsions. A similar study was also performed by Zhang et al. [137], who successfully prepared an emulsion with a droplet size of 27 nm that exhibited admirable physical stability for 8 months. They also found that the average droplet size of the emulsion decreased with an increase of the inlet pressure, the number of cavitation passes, and the surfactant concentration.

4. The hydrodynamic cavitation reactor

An HCR is designed to purposely initiate cavitation events in a controlled environment and then to utilize the energy generated by imploding cavitation bubbles to promote a variety of physical processes or chemical transformations. These devices can be used either as a stand-alone unit or in combination with other industrial processes. Two main types of HCR are reported in the literature and in today's market: stationary and rotational HCRs, which are reviewed in the following sections.

4.1. Stationary HCRs

Stationary HCRs employ venturis or orifices as the constrictive part to increase the linear velocity of the working fluid, which leads to a low-pressure region where cavitation events are induced. Due to their simple geometry and ease of fabrication and operation, stationary HCRs have been extensively studied and widely used at the laboratory scale to research the effectiveness and mechanism of hydrodynamic cavitation technology. Because of the considerable pressure drop of the working fluid caused by the contractive parts, a powerful pump is often required, which may result in a substantial cost.

Constriction is a critical part of a stationary HCR. Its geometry has a direct impact on both the generation of cavities and the pressure pulse produced in the process. Constriction also affects the pressure distribution along the flow path and hence the cavitation intensity. Moholkar and Pandit [138] performed a theoretical study to understand the effect of constriction geometry on cavitation intensity. Both venturis and orifice plates were studied and compared. The researchers found that the radial bubble motion in a venturi was due to the linear pressure recovery gradient, and that the bubble motion in the orifice flow was a combination of stable oscillatory motion and transient motion. Furthermore, the magnitude of the pressure drop across the orifice plate was much higher than that in venturi tubes; as such, the cavitation intensity produced by the orifice plate had a much higher magnitude than that produced by a venturi. This finding was confirmed by Ozonek [139]. In addition, the constriction-related parameters of the cavitating device have been found to significantly influence the inception and intensity of hydrodynamic cavitation. The design of venturis and orifice plates are reviewed in the following sections.

4.1.1. Orifice plate cavitation reactor

An orifice plate is the most commonly used pressure-reducing and flow-restricting device, and includes a borehole that is designed to generate a specified pressurized flow. Due to the sudden change in pipe diameter, the intensity of the bubble collapse produced at an orifice is significant. The generation of bubbles occurs at the edge of the orifice. To increase the edges, multiple orifice plates have been designed. Boundary layer separation occurs during the passage of the liquid, and a huge amount of energy is lost in the form of permanent pressure drop. The magnitude of the pressure drop greatly influences the intensity of turbulence downstream of the constriction, and the pressure drop mainly depends on the geometry of the constriction and the flow

conditions of the liquid. A typical pressure profile of an orifice plate cavitating device is shown in Fig. 7 [140], where p_1 is the upstream pressure, p_2 is the recovered downstream pressure, and p_v is the vapor pressure of the fluid.

The diameter of the constriction is one of the most important factors in orifice design and can significantly affect the generation of cavitation. An example is shown in Fig. 8 [141]. Yan and Thorpe [17] studied both experimental and theoretical aspects of the flow regime transitions induced by cavitation, where water passed through orifices with different sizes. They observed that the cavitation number exhibited an approximately linear increase with the increase of the orifice diameter. Similar results were obtained by other research groups [22,108,142–144]. The collapse pressure generated by a single cavity has also been found to increase with increasing orifice diameter. Ai and Ding [145] studied the orifice plate cavitation mechanism and its influencing factors using a numerical model. They found that the cavitation induced by the orifice plate was strongly related to the gas nucleus distribution and the contraction ratio: The larger the contraction ratio, the higher the intensity of cavitation.

The flow area is the total cross-sectional area for a liquid to flow inside a cavitating device; it is also a factor that is associated with cavitation intensity. Amin et al. [118] studied the optimization of hydrodynamic cavitation using salicylic acid and stated that the concentration of free radicals generated inversely correlated with flow area. This result suggests that the intensity of cavitation decreases with increasing flow area. In agreement with this statement, a simulation by Simpson and Ranade [146] demonstrated that an increase in the orifice's flow area led to a lower fluid velocity at the constriction, which resulted in slower pressure recovery downstream and an increase in the cavitation number. Ghayal et al. [147] used α (the ratio of the total perimeter of holes to the total flow area on the plate) as a criterion to measure cavitation intensity. They reported that a plate with multiple holes and a smaller hole size, and thus a higher α value, was effective in producing a better cavitation effect. However, a contradictory result was obtained by Huang et al. [148], who found that the degradation rate of chitosan was increased with a larger flow area, due to the enlarged cavitation region.

As cavities can only be formed along the periphery of the holes, a plate with multiple holes should be considered during the design of an orifice-based cavitation reactor in order to produce higher cavitation intensity. The quantity, size, and shape of these holes must be considered. Compared with a single-hole plate, an orifice
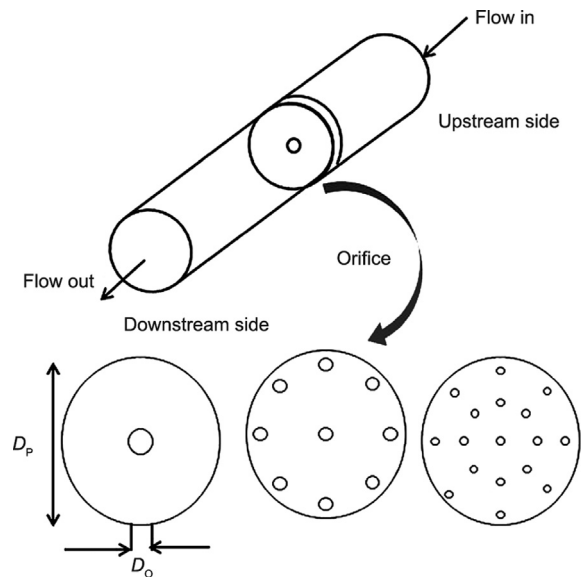

Fig. 8. Illustration of a different orifice design. D_O: diameter of orifice; D_P: diameter of plate. Reproduced from Ref. [141] with permission.

plate with multiple holes can generate more cavities due to the larger orifice perimeter. Due to its importance, orifice design has been subjected to extensive research. Sivakumar and Pandit [149] employed a multi-hole orifice cavitation reactor to degrade a rhodamine B aqueous solution. They found that the efficiency of the degradation significantly improved due to the smaller sized openings. Rudolf et al. [150] experimentally investigated the effectiveness of different orifice geometries. Compared with a single-hole orifice, they found multi-hole orifices to have a much lower energy dissipation; thus, they concluded that it is more effective to use multi-hole orifices. Senthil Kumar et al. [151] used a multi-hole HCR to decompose an aqueous KI solution; their results showed that the iodine liberation rates were three times higher than acoustic cavitation under the same power dissipation rates. Similar results were confirmed by Kalumuck and Chahine [152]. Instead of an orifice with simple geometry, they created multiple zones of hydrodynamic cavitation in a recirculatory pipe for the degradation of p-nitrophenol. Their study demonstrated that focusing on a combination of the geometric design of the orifice and the operating conditions was an appropriate approach to optimize hydrodynamic cavitation intensity with minimum energy consumption. Bagade et al. [153] reviewed several flow characteristics and design methodologies regarding multi-hole orifice plates using both theoretical and experimental analysis methods. They concluded that an orifice plate with multiple holes is more effective than a single-hole orifice in terms of intensity and desired transformation.

4.1.2. Venturi cavitation reactor

Venturi tubes have been extensively used and studied as a way to produce microbubbles in cavitation processes. A venturi tube typically consists of three sections: the converging inlet, throat, and divergent cone. Unlike orifice plates, the fluid inside a venturi contracts and expands smoothly; therefore, the fluid pressure and velocity vary consistently. This gradual change in the fluid conditions avoids a dramatic change in orifice pressure, which is beneficial for the generation of microbubbles and their stability. Due to its lower energy consumption and higher bubble generation ability, venturis surpass orifice plates in industrial applications [154].

Similar to an orifice plate cavitation reactor, the geometry of a venturi in a venturi cavitation reactor can impact the overall performance (Fig. 9) [155]. The outlet angle of the venturi has been
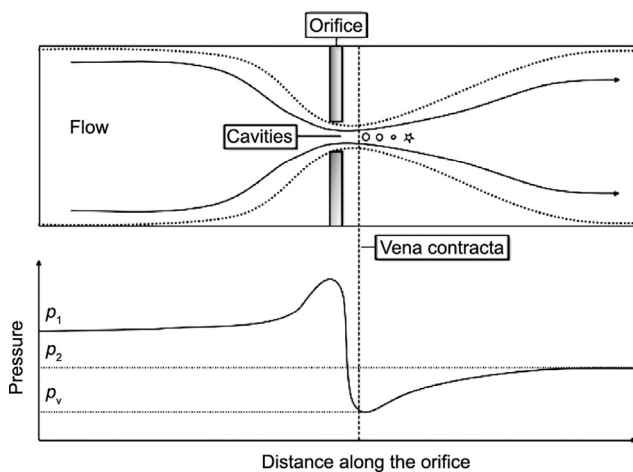

Fig. 7. Illustration of an orifice plate with a pressure profile. p_1: upstream pressure; p_2: recovered downstream pressure; p_v: vapor pressure of the fluid. Reproduced from Ref. [140].

found to be one of the main geometric parameters affecting the operation characteristics. Bashir et al. [156] performed a theoretical analysis on four venturis with different outlet angles and stated that the outlet angles of the divergence section control the rate of cavity collapse. The optimum divergence angle was found to be 5.5°, as the cavitation number obtained at 5.5° was the lowest among those four. Ulas [157] recommended using a 7° diverging angle to minimize the pressure loss during cavitation processes. Based on that, Ashrafizadeh and Ghassemi [158] investigated the hydrodynamic cavitation performance with four different diffuser angles of 5°, 7°, 10°, and 15°. Their results showed that increasing the diffuser angle leads to a decrease in the critical pressure ratio from 0.75 to around 0.6 and to a narrower cavitating region, which is not favorable. Similar results were obtained by Brinkhorst et al. [159], who found that a larger outlet angle lowered the cavitation intensity, as a higher diffuser angle corresponded to earlier flow separation, resulting in low bubble generation and collision efficiency. Therefore, a larger outlet angle is usually not favorable for stable cavitation. Li et al. [160] also suggested that lowering the outlet angle is an efficient way to produce more microbubbles and reduce the flow resistance during a cavitation process.

The throat is another essential component of a venturi, as the bubbles are generated at the throat. The length of the throat is a structural parameter that must be considered for its effectiveness in generating cavitation. Ashrafizadeh and Ghassemi [158] studied the impact of different throat lengths (1.0, 1.5, 2.0, and 2.5 mm) on the generation of cavities. Their results showed that increasing the throat length from 1.0 to 2.5 mm reduced the number of cavities generated, but energy dissipation was surpassed due to friction. Saharan et al. [154] studied the throat perimeter against the effectiveness of the degradation of dyes using two different types of venturis. Their result showed that a slit venturi yields a higher degradation percentage than a circular venturi. Similar results were obtained by Bashir et al. [156], whose CFD analysis suggested that a throat height-to-length ratio of 1:1 gives the greatest cavitation effect, as compared with others with a ratio of 1:0.5, 1:2, and 1:3. Bimestre et al. [161] theoretically and experimentally investigated how venturi-based cavitation affects the pretreatment of sugarcane bagasse. They observed that the cavitation number decreased with an increase in throat length (1.5, 3.0, and 5.0 mm) and increased with increasing throat diameter (1.5 and 2.0 mm). Kuldeep and Saharan [162] compared the performance of a venturi and an orifice via computational analysis. Their result indicated that a 1:1 ratio of throat diameter to length and a 6.5° divergence angle are optimal for a venturi-type cavitation reactor, while an orifice diameter-to-length ratio of 1:3 is the most suitable value for an orifice plate reactor.

4.2. Rotational HCRs

In contrast to stationary HCRs, rotational HCRs consist of rotational parts that generate cavitation. Early rotational HCRs used high-speed impellers or other sharp blades to accelerate the tangential velocity of the fluid, so that the local pressures were reduced below the vapor pressure and cavitation was generated. Instead of impellers, recently reported rotational HCRs use circular disks or cylinders with numerous dimples or gaps to create cavitation. The uneven surfaces (due to dimples or gaps) within the rotational part create variations in the working cross-sectional area, which forces the liquid fluid to expand or contract as it flows through the area. Repeating pressure differentials are thus produced. In order to uniformly distribute the liquid stream, the inlet port is located at the center and the outlet port is placed at the top of the shaft for sealing and cooling purposes. Cavitation generated from this process is due to the opposite movement of two shear layers; therefore, this type of cavitation is also called shear cavitation [163]. A graphic illustration of a rotational cavitation reactor is provided in Fig. 10 [164].

With different cavitation generation mechanisms, rotational HCRs eliminate the pressure fluctuations that are the inherent drawback of stationary HCRs. However, the movable parts in rotational HCRs are expected to need frequent maintenance. For a rotational HCR, the rotational speed of the rotor, liquid flow rate, and pressures are of importance in determining the overall performance [81]. The rotational speed of the reactor is a determining factor. A critical rotational speed exists, which is the threshold of cavitation generation. A higher rotational speed produces higher tangential fluid velocity, which leads to higher turbulence intensity and lower system pressure. This was confirmed by Jyoti and Pandit [165], who applied a rotational HCR to disinfect bacteria in well water. Rotational speeds of 4000, 8000, and 12 000 were tested, and bacteria-removal rates of 3.7%, 61.5%, and 96%, respectively, were recorded. Increased cavitation intensity was responsible for the enhanced disinfection rate. The positive effect of rotation rate was further verified by recently published results. Sun et al. [166] evaluated the thermal performance of a rotational HCR against the rotational speed of the reactor rotor. As the rotor speed increased from 2700 to 3600 $r \cdot min^{-1}$, the heat generation rates were observed to significantly increase. Unfortunately, the effect of rotational speed was not differentiated from other factors such as flow rate and pressure. The same research group applied the same rotational HCR to disinfect water by killing $E.\ coli$. Their work confirmed the positive effects of rotational speed and supported the finding that the liquid flow rate also plays a key role in enhancing cavitation intensity. Sun et al. [81] increased the water flow rate from 8 to 11 $L \cdot min^{-1}$ at a fixed rotational speed of 3600 $r \cdot min^{-1}$, and found that the removal rate of $E.\ coli$ improved from 35.43% to 100%. The boosted disinfection rate was a result of the increased cavitation intensity, which was induced by the increased liquid flow rate. The researchers suggested that more nuclei were entrapped in the water as the flow rate increased, which was the root cause of the enhanced intensity of cavitation.
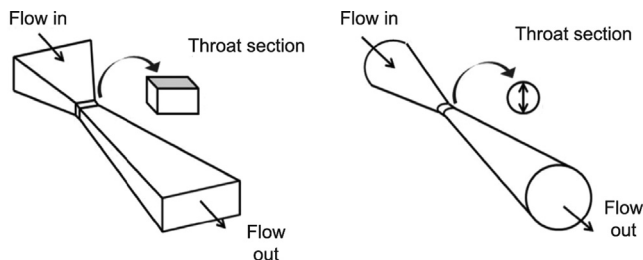

Fig. 9. Illustration of the geometric design of different venturis. Reproduced from Ref. [155].
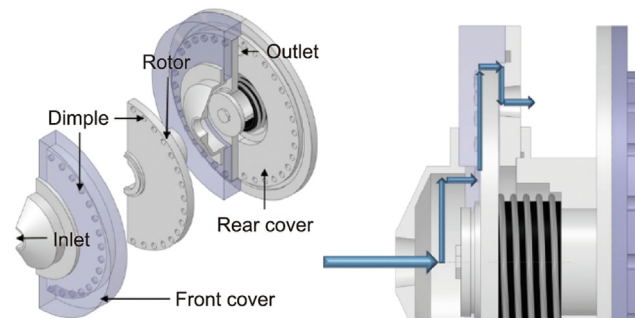

Fig. 10. Graphic illustration of a rotational cavitation reactor. Reproduced from Ref. [164] with permission.

Šarc et al. [167] used different types of cavitation to remove bacteria and stated that exposure to supercavitation efficiently destroyed the bacteria, while acoustic and developed hydrodynamic cavitation only marginally reduced the viable bacterial count. The performance of supercavitation was found to be about 100 times better in terms of electric energy cost.

4.2.1. Application and scalability

Rotational HCRs have been applied in various chemical processes. Crudo et al. [168] applied this type of reactor to produce biodiesel. They stated that the fatty acid methyl ester conversion rate was greater than 99% m/m, while the energy consumption required to produce biodiesel was only 0.015 kW·h·L^{-1}. Maršálek et al. [169] performed an experimental study using a rotational cavitation reactor to remove cyanobacteria from wastewater. They stated that 99% of the cyanobacteria was removed from water with the addition of 0.1 mmol H$_2$O$_2$ in just 10 s, along with 98% inhibition of photosynthesis with no cell destruction. Badve et al. [114] used a rotational HCR in an organic wastewater treatment process and found that the degradation of organic matter was dependent on the speed of the rotor. Patil et al. [170] used a rotational HCR to intensify the production of biogas and reported an increase of almost 100% under optimized treatment.

The discussion of scalability will be focused on rotational HCRs. According to various studies, rotation-based cavitation reactors have shown promising cavitation effectiveness. However, in order to scale up and optimize a rotational cavitation reactor, it is necessary to thoroughly understand the geometric and operational parameters, as well as the capital and operational costs.

Šarc et al. [171] obtained a disinfection rate of 99.95% and a treatment rate of 0.013 L·min^{-1} with a cost of 18.2 USD·m^{-3}. A similar outcome was reported by Loraine et al. [172], who proposed a device that was 10–100 times more efficient than ultrasonic disinfection in terms of energy efficiency. Moreover, when the reactor was up-scaled from the laboratory scale to the pilot scale, it showed a significant improvement in terms of efficiency and cost. Sun et al. [173] performed a comprehensive study using this novel reactor for disinfection at the pilot scale. They found that the treatment rate increased by 300 times with just one-tenth of the cost in comparison with the device proposed by Loraine et al. [172], and increased by 140 times and was 50 times more economically efficient compared with the laboratory scaled device proposed by Cerecedo et al. [174]. Many other studies have been conducted at the laboratory scale [15,175–178].

Pilot-scale rotational cavitating devices have been built based on the successful operation of laboratory-scale equipment and have shown promising cavitational effects and economic viability. Petkovšek et al. [179] used a rotational type of reactor in both water treatment and sludge disintegration processes. The soluble COD of waste-activated sludge increased from 45 to 602 mg·L^{-1} after 20 passes through the rotation generator of hydrodynamic cavitation, and biogas production also increased by to about 12.7%. Sežun et al. [180] used the advantages of a rotational cavitation reactor to enhance nutrient release from secondary pulp and paper mill sludge. The results showed an increase in soluble COD of 2400 mg·L^{-1} and in total nitrogen of 120 mg·L^{-1} with the addition of NaOH. Moreover, the cost of 1.9 kg of released soluble COD from alkaline pretreatment and cavitated sludge was only one euro. Kovačič et al. [181] reported the effectiveness of a rotational cavitation device on the removal of bisphenols and other containments at the pilot scale. The highest removal efficiency obtained was 90% at a rotational speed of 2290 r·min^{-1}, and the researchers confirmed the potential of hydrodynamic cavitation as a pretreatment process for large-scale application. A comprehensive comparison of recently reported rotational cavitation reactors on two scales is shown in Table 3 [15,81,171,173–181].

The cavitation induced by a stationary HCR has been extensively studied at different scales due to the unique advantages of such reactors, which include ease of operation and simple structural design. With these dominant features, stationary HCRs have been successfully applied in various industrial fields. However, studies have not yet been extensively conducted on rotor-type reactors, which has significantly delayed the development of their application. Furthermore, a rotor-based reactor produces a significant amount of energy in the form of heat during operation. Therefore, the development of high-efficiency rotational cavitation reactors is the key when moving from the laboratory scale to a larger scale and to commercialized applications. The rotational cavitation reactor generates not only cavities but also shear stress, due to the high-speed rotation of the impeller. Cavitation and shear stress can synergistically enhance the reactions that take place in a rotational cavitation reactor. In addition, both the dimensions of the cylindrical rotor and the geometrical structure of a rotational cavitation reactors can be easily adjusted or scaled up to meet the specified requirements. Good scalability and space utilization make them suitable for large-scale applications [182].

4.2.2. Commercial reactors

Due to its advantages, such as low capital and operational cost, shorter production time, enhanced production, and efficiency, hydrodynamic cavitation has been successfully applied in many industrial fields, including oil refining, petroleum upgrading, industrial water treatment, biodiesel production, gas–liquid mixing, and hydrocarbon upgrading. A few companies and their corresponding reactors that are based on cavitation technology are summarized in this section.

Cavitation Technologies, Inc. is an innovative company that focuses on processing liquids, fluidic mixtures, and emulsions and owns a patented technology named the CTi Nano Neutralization process, which is a multi-stage hydrodynamic cavitation device. The reaction system is flexible in scale and can serve both large-scale and small-scale producers in the fields of edible oil refining, algal oil extraction, renewable fuel production, biodiesel production, alcoholic beverage enhancement, water treatment, and petroleum upgrading.

Hydro Dynamics, Inc. has developed a ShockWave Power Reactor, claiming that it "controls cavitation." The core technology of the device is a specially designed rotor. The spinning action generates hydrodynamic cavitation in the rotor cavities away from the metal surfaces; therefore, there is no damage. The company claimed that the ShockWave Power Reactor was featured by its relatively low capital and maintenance expenditures and its improved efficiency. The reactor has been installed all over the world to fulfil the needs of breweries, the production of renewable fuels, and the mixing, extraction, emulsification, oxidation, and petroleum industries; it has also been used by several Fortune 500 companies.

Mitton Cavitation, Inc. proposed a cavitational reactor that incorporated a small, robust, high-efficiency reactor to control the power of cavitation without suffering from its effects. A Mitton Cavitation Reactor is an applied cavitation reactor system that can be applied to the industrial scale, for treating approximately 1000 gal (1 gal = 3.785 L) of liquid using just 1 kW of energy. Its stackable design makes it upwardly scalable, and it can operate under both positive and negative pressure with intense molecular pressure, heat, and shear.

CaviMax, Inc. is a leading UK supplier of hydrodynamic cavitation devices. This corporation invented the rotational CaviMax cavitator to maximize the production potential of cavitation for various industrial applications such as biodiesel production, biomass pretreatment, sustainable chemical reactions, and even the cosmetics industry. The Rotocav reactor at the heart of the

Table 3
Summary of rotational cavitation reactors with handled volume up to 60 and 500 L.

Scale	Application	Experimental parameters	Findings	Ref.
Lab scale	Microorganism inactivation	Treatment rate: 0.013 L·min^{-1}; test volume: 2 L; disinfection rate: 99.95%; cavitation number: 0.78–1.57	Rotation generator proved to be economically and microbiologically far more effective than classical venturi section cavitation	[171]
	Water disinfection	Treatment rate: 4.3 L·min^{-1}; test volume: 60 L; disinfection rate: 100%	Disinfection rate of water was significantly enhanced	[81]
	Water disinfection	Treatment rate: 0.032 L·min^{-1}; test volume: 0.25 L; disinfection rate: 100%	Rotational cavitation reactors are two orders of magnitude more energy efficient than conventional ones	[174]
	Paper production	Rotational speed: 1 000, 5 400, 6 000 r·min^{-1}; cavitation number: 43.6, 1.2 and 0.7	Proved to be economically feasible in comparison with the laboratory scale	[178]
	Sludge treatment	Test volume: 40 L (laboratory scale) and 615 L (industrial scale); flow rate: 40 to 300 L·min^{-1}	Both specific energy of sludge solubilization (SE$_{SCOD}$) (decreased from 271 to 16 kJ·g^{-1}) and specific energy (decreased from 35 800 to 2 850 kJ·kg^{-1}) decreased when cavitation is scaled from laboratory scale to industrial scale	[177]
	Water recycling	Rotational speed: 10 000 r·min^{-1}; flow rate: 1.8 L·min^{-1}	22% reduction in COD and 37% increase in the redox potential, sediments reduced by 50%, and insoluble particles by 67%; four times more energy efficient compared with a venturi design	[175]
	Pharmaceutical removal	Rotational speed: 2 800 r·min^{-1}; motor power: 0.37 kW	Over 80% effect was achieved	[15]
	Wastewater treatment	Treatment time: 30 min; temperature: 50 °C; 340 mg·L^{-1} of added H$_2$O$_2$	Removes up to 79% of wastewater effluent; shear-induced cavitation is more efficient than cavitation by venturi	[176]
Pilot scale	Sludge disintegration	Rotational speed: 1 740, 2 290, 2 850 r·min^{-1}	SCOD increased from 45 to 602 mg·L^{-1} and 12.7% more biogas produced	[179]
	Wastewater management	400 W electrical motor; rotational speed: 10 000; sludge pH prior to cavitation: 10	Increased soluble COD by 2 400 mg·L^{-1}, total nitrogen by 120 mg·L^{-1}, and total phosphorous by 2.3 mg·L^{-1}; cost of only one euro per 1.9 kg of sludge	[180]
	Contaminant removal	Rotational speed: 2 290, 2 700 r·min^{-1}; treatment time: 10 min	Removal efficiencies for bisphenols are 15%–90%; showed potential for large-scale application	[181]
	Water treatment	Treatment rate: 4.5 L·min^{-1}; test volume: 18 L; disinfection rate: 100%	Treatment rate 140 times higher than other rotational cavitation reactor, 50 times lower expenses	[173]

SCOD: soluble chemical oxygen demand.

CaviMax can produce physical rotation forces that create shockwaves, breaking down incompatible mixtures into a flowing substrate. It has the potential to increase the yield by up to 20%, with remarkably little energy required.

A novel hydrodynamic cavitation device based on a vortex diode (VodCa®) has been developed and commercialized [183]. This device is designed to create a strong vortex flow, where the tangential forces are used to generate cavitation. It has been applied in various fields, including wastewater treatment, biogas production, biological digesters, and disinfection [184–186].

5. Concluding remarks and perspectives

Since cavitation first became known to the world due to its powerful potential for destruction, tremendous research efforts have been made to fundamentally understand the formation, intensity, and detrimental effects of cavitation. Researchers soon began to explore how to harvest the energy released by the implosion of cavitation bubbles and how to make good use of this unique phenomenon. To date, cavitation technology has drawn a great deal of attention for the energy-efficient intensification of various physical and chemical processes.

Cavitation is a complex phenomenon. Although much has been accomplished, many fundamental details of hydrodynamic cavitation are still not understood. Extensive research efforts have been made to study cavitation formation and development in an open water system and in a pump system. Such findings are often directly applied to a closed system, such as a cavitation reactor. The extrapolation has its inherent limitation. Thus, it is not surprising to observe a discrepancy in the determination of cavitation number, which is an important parameter characterizing cavitating flow. The pressures and velocities in the upstream, in the downstream, and at the constriction have been applied to determine the cavitation number, and the comparability of results among the published reports has greatly suffered as a result.

To apply cavitation technology to various processes and to design an appropriate cavitation reactor, a fundamental understanding of the inception of cavitation and the hydrodynamics of cavitation flow in a closed reaction system is essential. Thus, more efforts are urged to make on the hydrodynamics of cavitating flow. This knowledge will facilitate the design of a highly efficient cavitation reactor, in which the inception of cavitation and the development of intensive cavitation can be realized at the expense of low external energy. Recent achievements in determining the influencing factors of cavitation formation and the bubble nucleation process provide a firm scientific basis for such an endeavor. The configuration of the constriction should be considered in order to generate desirable cavitation. Seeding nuclei in the liquid flow can significantly reduce the tensile strength of the liquid required for forming cavitation. In addition, operating conditions such as the fluid temperature and pressure, as well as the physical properties of the liquid stream, can affect cavitation and must be considered in order to achieve the optimum outcome. This understanding encourages researchers to design optimal cavitation reactors that maximize positive outcomes.

This review systematically examined two different types of HCR from the lab scale and pilot scale to the commercial scale. Although hydrodynamic cavitation is considered to be a cost-effective and energy-efficient technique that is seeing an exponential increase in applications, scaling up cavitation-based processes remains a major challenge due to a lack of reliable models for the prediction of cavitation and poorly understood scale-up processes from the bench to commercialization.

Cavitation provides unparalleled advantages over its conventional counterpart technologies. The implosion of cavitation bubbles generates hot spots accompanied by extreme high temperatures and pressures, where radicals and UV radiation are produced. Based on the advantages of cavitation, researchers have widely applied cavitation technology to various chemical processes, such as biofuel production, advanced oxidization processes (AOPs), bioactive extraction, pollutant degradation, and

microorganism disinfection. Cavitation has been extensively studied in AOPs. Without the addition of chemicals, the cavitation process can generate a significant amount of highly reactive radicals such as OH·, O·, and HOO·, which can remove the organic contaminates present in water and wastewater effluent in the form of mineral end products and carbon dioxide. In the treatment of water and wastewater streams, cavitation technology can be applied in order to avoid the use of chemicals and treat a large quantity of effluents in an efficient, economical, and energy-saving way. Aside from chemically active radicals, the extreme local temperature and pressure that result from cavitation present a distinct microenvironment that promotes chemical reactions. This was evidenced by Chuah et al. [130], who demonstrated that the rate constants of the conversion of vegetable oil to biodiesel in a cavitation-based process were significantly higher than those in a mechanical stirring reactor. In addition, cavitation technology has been demonstrated to be effective in enhancing mass transfer. It is anticipated that cavitation technology holds great potential for enhancing heterogeneous catalytic reactions. Unfortunately, few studies have documented this subject.

In summary, hydrodynamic cavitation is an emerging technology that has been used to intensify a variety of chemical and physical processes. This work comprehensively reviewed the fundamentals of cavitation, the optimization and effective design of cavitation reactors, commercial cavitation reactors on the market, and applications of such reactors at the lab and pilot scales.

Acknowledgments

Compliance with ethics guidelines

Haoxuan Zheng, Ying Zheng, and Jesse Zhu declare that they have no conflict of interest or financial conflicts to disclose.

References

[1] Suslick KS. Sonochemistry. Science 1990;247(4949):1439–45.
[2] Tao Y, Cai J, Huai X, Liu B, Guo Z. Application of hydrodynamic cavitation to wastewater treatment. Chem Eng Technol 2016;39(8):1363–76.
[3] Asaithambi N, Singha P, Dwivedi M, Singh SK. Hydrodynamic cavitation and its application in food and beverage industry: a review. J Food Process Eng 2019;42(5):e13144.
[4] Brujan E. Cavitation in non-Newtonian fluids: with biomedical and bioengineering applications. Berlin: Springer Science + Business Media; 2011.
[5] Gogate PR, Pandit AB. Hydrodynamic cavitation reactors: a state of the art review. Rev Chem Eng 2001;17(1):1–85.
[6] Lauterborn W. Cavitation and coherent optics. In: Lauterborn W, editor. Cavitation and inhomogeneities in underwater acoustics. Berlin: Springer; 1980. p. 3–12.
[7] Lauterborn W, Bolle H. Experimental investigations of cavitation-bubble collapse in the neighbourhood of a solid boundary. J Fluid Mech 1975;72(2):391–9.
[8] Shah YT, Pandit AB, Moholkar VS. Cavitation reaction engineering. New York City: Kluwer Academic/Plenum Publishers; 1999.
[9] Moholkar VS, Senthil Kumar P, Pandit AB. Hydrodynamic cavitation for sonochemical effects. Ultrason Sonochem 1999;6(1–2):53–65.
[10] Gogate PR. Greener processing routes for reactions and separations based on use of ultrasound and hydrodynamic cavitation. In: Stefanidis G, Stankiewicz A, editors. Alternative energy sources for green chemistry. London: Royal Society of Chemistry; 2016. p. 126–60.
[11] Holkar CR, Jadhav AJ, Pinjari DV, Pandit AB. Cavitationally driven transformations: a technique of process intensification. Ind Eng Chem Res 2019;58(15):5797–819.
[12] Šarc A, Stepišnik-Perdih T, Petkovšek M, Dular M. The issue of cavitation number value in studies of water treatment by hydrodynamic cavitation. Ultrason Sonochem 2017;34:51–9.
[13] Föttinger H. Untersuchungen über Kavitation und Korrosion bei Turbinen, Turbopumpen und Propellern. In: Wissenschaftlicher Beirat des Vereines

Deutscher Ingenieure, editor. Hydraulische Probleme. Berlin: VDI-Verlag; 1926. p. 14–64. German.
[14] Plesset MS. The dynamics of cavitation bubbles. J Appl Mech 1949;16(3):277–82.
[15] Petkovšek M, Zupanc M, Dular M, Kosjek T, Heath E, Kompare B, et al. Rotation generator of hydrodynamic cavitation for water treatment. Separ Purif Tech 2013;118:415–23.
[16] Bagal MV, Gogate PR. Wastewater treatment using hybrid treatment schemes based on cavitation and Fenton chemistry: a review. Ultrason Sonochem 2014;21(1):1–14.
[17] Yan Y, Thorpe RB. Flow regime transitions due to cavitation in the flow through an orifice. Int J Multiph Flow 1990;16(6):1023–45.
[18] Cioncolini A, Scenini F, Duff J, Szolcek M, Curioni M. Choked cavitation in micro-orifices: an experimental study. Exp Therm Fluid Sci 2016;74:49–57.
[19] Cheng X, Shao X, Zhang L. The characteristics of unsteady cavitation around a sphere. Phys Fluids 2019;31(4):042103.
[20] Long X, Zhang J, Wang J, Xu M, Lyu Q, Ji B. Experimental investigation of the global cavitation dynamic behavior in a venturi tube with special emphasis on the cavity length variation. Int J Multiph Flow 2017;89:290–8.
[21] Ghorbani M, Sadaghiani AK, Villanueva LG, Koşar A. Hydrodynamic cavitation in microfluidic devices with roughened surfaces. J Micromech Microeng 2018;28(7):075016.
[22] Balasundaram B, Harrison STL. Disruption of Brewers' yeast by hydrodynamic cavitation: process variables and their influence on selective release. Biotechnol Bioeng 2006;94(2):303–11.
[23] Saharan VK, Badve MP, Pandit AB. Degradation of Reactive Red 120 dye using hydrodynamic cavitation. Chem Eng J 2011;178:100–7.
[24] Soyama H. Luminescence intensity of vortex cavitation in a venturi tube changing with cavitation number. Ultrason Sonochem 2021;71:105389.
[25] Carpenter J, George S, Saharan VK. Low pressure hydrodynamic cavitating device for producing highly stable oil in water emulsion: effect of geometry and cavitation number. Chem Eng Process 2017;116:97–104.
[26] Pelz PF, Keil T, Groß TF. The transition from sheet to cloud cavitation. J Fluid Mech 2017;817:439–54.
[27] Ramamurthi K, Patnaik S. Influence of periodic disturbances on inception of cavitation in sharp-edged orifices. Exp Fluids 2002;33(5):720–7.
[28] Dular M, Bachert B, Stoffel B, Širok B. Relationship between cavitation structures and cavitation damage. Wear 2004;257(11):1176–84.
[29] Hatano S, Kang D, Kagawa S, Nohmi M, Yokota K. Study of cavitation instabilities in double-suction centrifugal pump. Int J Fluid Mach Syst 2014;7(3):94–100.
[30] Keller AP. Cavitation scale effects—empirically found relations and the correlation of cavitation number and hydrodynamic coefficients. In: CAV 2001: Fourth International Symposium on Cavitation; 2001 Jun 20–23; Pasadena, CA, USA; 2001.
[31] Ando K, Liu AQ, Ohl CD. Homogeneous nucleation in water in microfluidic channels. Phys Rev Lett 2012;109(4):044501.
[32] Mørch KA. Cavitation inception from bubble nuclei. Interface Focus 2015;5(5):20150006.
[33] Groß TF, Pelz PF. Diffusion-driven nucleation from surface nuclei in hydrodynamic cavitation. J Fluid Mech 2017;830:138–64.
[34] Khoo MT, Venning JA, Pearce BW, Takahashi K, Mori T, Brandner PA. Natural nuclei population dynamics in cavitation tunnels. Exp Fluids 2020;61(2):34.
[35] Fox FE, Herzfeld KF. Gas bubbles with organic skin as cavitation nuclei. J Acoust Soc Am 1954;26:984–9.
[36] Hsiao CT, Chahine GL. Effect of a propeller and gas diffusion on bubble nuclei distribution in a liquid. J Hydrodyn 2012;24:809–22.
[37] Tandiono T, Kang CW, Lu X, Turangan CK, Tan M, Osman HB, et al. An experimental study of gas nuclei-assisted hydrodynamic cavitation for aquaculture water treatment. J Vis 2020;23(5):863–72.
[38] Russell PS, Barbaca L, Venning JA, Pearce BW, Brandner PA. Measurement of nuclei seeding in hydrodynamic test facilities. Exp Fluids 2020;61(3):79.
[39] Pascal RW, Yelland MJ, Srokosz MA, Moat BI, Waugh EM, Comben DH, et al. A spar buoy for high-frequency wave measurements and detection of wave breaking in the open ocean. J Atmos Ocean Technol 2011;28(4):590–605.
[40] Yao X, Li Z, Sun L, Lu H. A study on bubble nuclei population dynamics under reduced pressure. Phys Fluids 2020;32(11):112019.
[41] Hemmingsen EA. Cavitation in gas-supersaturated solutions. J Appl Phys 1975;46(1):213–8.
[42] Venning JA, Khoo MT, Pearce BW, Brandner PA. Background nuclei measurements and implications for cavitation inception in hydrodynamic test facilities. Exp Fluids 2018;59(4):71.
[43] Johnson BD, Cooke RC. Generation of stabilized microbubbles in seawater. Science 1981;213(4504):209–11.
[44] Calgaroto S, Wilberg KQ, Rubio J. On the nanobubbles interfacial properties and future applications in flotation. Miner Eng 2014;60:33–40.
[45] Etcheparè R, Oliveira H, Nicknig M, Azevedo A, Rubio J. Nanobubbles: generation using a multiphase pump, properties and features in flotation. Miner Eng 2017;112:19–26.
[46] Ohgaki K, Khanh NQ, Joden Y, Tsuji A, Nakagawa T. Physicochemical approach to nanobubble solutions. Chem Eng Sci 2010;65(3):1296–300.
[47] Jin F, Li J, Ye X, Wu C. Effects of pH and ionic strength on the stability of nanobubbles in aqueous solutions of α-cyclodextrin. J Phys Chem B 2007;111(40):11745–9.
[48] Azevedo A, Etcheparè R, Calgaroto S, Rubio J. Aqueous dispersions of nanobubbles: generation, properties and features. Miner Eng 2016;94:29–37.

[49] Pourkarimi Z, Rezai B, Noaparast N. Effective parameters on generation of nanobubbles by cavitation method for froth flotation applications. Physicochem Probl Miner Process 2017;53(2):920–42.

[50] Phan KKT, Truong T, Wang Y, Bhandari B. Nanobubbles: fundamental characteristics and applications in food processing. Trends Food Sci Technol 2020;95:118–30.

[51] Michailidi ED, Bomis G, Varoutoglou A, Efthimiadou EK, Mitropoulos AC, Favvas EP. Fundamentals and applications of nanobubbles. In: Kyzas GZ, Mitropoulos AC, editors. Interface science and technology. Volume 30. Advanced low-cost separation techniques in interface science. London: Academic Press; 2019. p. 69–99.

[52] Xiong R, Xu RX, Huang C, De Smedt S, Braeckmans K. Stimuli-responsive nanobubbles for biomedical applications. Chem Soc Rev 2021;50(9):5746–76.

[53] Zhou M, Cavalieri F, Caruso F, Ashokkumar M. Confinement of acoustic cavitation for the synthesis of protein-shelled nanobubbles for diagnostics and nucleic acid delivery. ACS Macro Lett 2012;1(7):853–6.

[54] Favvas EP, Kyzas GZ, Efthimiadou EK, Mitropoulos AC. Bulk nanobubbles, generation methods and potential applications. Curr Opin Colloid Interface Sci 2021;54:101455.

[55] Weijs JH, Seddon JRT, Lohse D. Diffusive shielding stabilizes bulk nanobubble clusters. ChemPhysChem 2012;13(8):2197–204.

[56] Yasui K, Tuziuti T, Kanematsu W, Kato K. Dynamic equilibrium model for a bulk nanobubble and a microbubble partly covered with hydrophobic material. Langmuir 2016;32(43):11101–10.

[57] Alheshibri M, Qian J, Jehannin M, Craig VSJ. A history of nanobubbles. Langmuir 2016;32(43):11086–100.

[58] Kim J, Song SJ. Measurement of temperature effects on cavitation in a turbopump inducer. J Fluids Eng 2016;138(1):011304.

[59] Niemczewski B. Observations of water cavitation intensity under practical ultrasonic cleaning conditions. Ultrason Sonochem 2007;14(1):13–8.

[60] Torre L, Cervone A, Pasini A, d'Agostino L. Experimental characterization of thermal cavitation effects on space rocket axial inducers. J Fluids Eng 2011; 133(11):111303.

[61] Li B, Gu Y, Chen M. An experimental study on the cavitation of water with dissolved gases. Exp Fluids 2017;58(12):164.

[62] De Giorgi MG, Ficarella A, Tarantino M. Evaluating cavitation regimes in an internal orifice at different temperatures using frequency analysis and visualization. Int J Heat Fluid Flow 2013;39:160–72.

[63] Joshi RK, Gogate PR. Degradation of dichlorvos using hydrodynamic cavitation based treatment strategies. Ultrason Sonochem 2012;19(3):532–9.

[64] Kumar PS, Pandit AB. Modeling hydrodynamic cavitation. Chem Eng Technol 1999;22(12):1017–27.

[65] Liu X, Wu Z, Li B, Zhao J, He J, Li W, et al. Influence of inlet pressure on cavitation characteristics in regulating valve. Eng Appl Comput Fluid Mech 2020;14(1):299–310.

[66] Liang J, Luo X, Liu Y, Li X, Shi T. A numerical investigation in effects of inlet pressure fluctuations on the flow and cavitation characteristics inside water hydraulic poppet valves. Int J Heat Mass Transf 2016;103: 684–700.

[67] Taşdemir A, Cengiz İ, Yildiz E, Bayhan YK. Investigation of ammonia stripping with a hydrodynamic cavitation reactor. Ultrason Sonochem 2020;60: 104741.

[68] Wu ZL, Ondruschka B, Bräutigam P. Degradation of chlorocarbons driven by hydrodynamic cavitation. Chem Eng Technol 2007;30:642–8.

[69] Flynn HG. Physics of acoustic cavitation in liquids. In: Mason WP, editor. Physical acoustics, Volume I—Part B. New York City: Academic Press Inc.; 1964. p. 57–172.

[70] Kim SJ, Lim KH, Kim CY. Deformation characteristics of spherical bubble collapse in Newtonian fluids near the wall using the finite element method with ALE formulation. Korea-Australia Rheol J 2006;18(2):109–18.

[71] Deng Q, Anilkumar AV, Wang TG. The role of viscosity and surface tension in bubble entrapment during drop impact onto a deep liquid pool. J Fluid Mech 2007;578:119–38.

[72] Luo J, Xu W, Zhai Y, Zhang Q. Experimental study on the mesoscale causes of the influence of viscosity on material erosion in a cavitation field. Ultrason Sonochem 2019;59:104699.

[73] Arndt REA. Cavitation in fluid machinery and hydraulic structures. Annu Rev Fluid Mech 1981;13:273–326.

[74] Nazari-Mahroo H, Pasandideh K, Navid HA, Sadighi-Bonabi R. How important is the liquid bulk viscosity effect on the dynamics of a single cavitation bubble? Ultrason Sonochem 2018;49:47–52.

[75] Li S, Brennen CE, Matsumoto Y. Introduction for amazing (cavitation) bubbles. Interface Focus 2015;5(5):20150059.

[76] Flint EB, Suslick KS. The temperature of cavitation. Science 1991;253(5026): 1397–9.

[77] Qin Z, Alehossein H. Heat transfer during cavitation bubble collapse. Appl Therm Eng 2016;105:1067–75.

[78] Zaporozhets EP, Kholpanov LP, Zibert GK, Artemov AV. Vortex and cavitation flows in hydraulic systems. Theor Found Chem Eng 2004;38(3):225–34.

[79] Little S. Null tests of breakthrough energy claims. In: Proceedings of the 42nd AIAA/ASME/SAE/ASEE Joint Propulsion Conference & Exhibit; 2006 Jul 9–12; Sacramento, CA, USA. Reston: American Institute of Aeronautics and Astronautics, Inc.; 2006.

[80] Pyun KB, Kwon WC, Oh KT, Yoon JY. Investigation of the performance for a heat generator using hydrodynamic cavitation. In: Proceedings of the ASME-JSME-KSME 2011 Joint Fluids Engineering Conference; 2011 Jul 24–29; Hamamatsu, Japan. New York City: American Society of Mechanical Engineers; 2011. p. 701–6.

[81] Sun X, Park JJ, Kim HS, Lee SH, Seong SJ, Om AS, et al. Experimental investigation of the thermal and disinfection performances of a novel hydrodynamic cavitation reactor. Ultrason Sonochem 2018;49:13–23.

[82] Song Y, Gu C. Development and validation of a three-dimensional computational fluid dynamics analysis for journal bearings considering cavitation and conjugate heat transfer. J Eng Gas Turbines Power 2015;137 (12):122502.

[83] Schneider B, Koşar A, Peles Y. Hydrodynamic cavitation and boiling in refrigerant (R-123) flow inside microchannels. Int J Heat Mass Transf 2007; 50(13–14):2838–54.

[84] Ghorbani M, Chen H, Villanueva LG, Grishenkov D, Koşar A. Intensifying cavitating flows in microfluidic devices with poly(vinyl alcohol) (PVA) microbubbles. Phys Fluids 2018;30(10):102001.

[85] Ghorbani M, Deprem G, Ozdemir E, Motezakker AR, Villanueva LG, Koşar A. On "cavitation on chip" in microfluidic devices with surface and sidewall roughness elements. J Microelectromech Syst 2019;28(5):890–9.

[86] Sole JD, Shelofsky BJ, Scaringe RP, Cole GS. Cavitation-enhanced microchannel heat exchanger demonstration and heat transfer correlation development using R-134a. In: Proceedings of the ASME 2012 Heat Transfer Summer Conferenc; 2012 Jul 8–12; Rio Grande, PR, USA. New York City: American Society of Mechanical Engineers; 2012. p. 607–15.

[87] Lee J, Mudawar I. Two-phase flow in high-heat-flux micro-channel heat sink for refrigeration cooling applications: part II—heat transfer characteristics. Int J Heat Mass Transf 2005;48(5):941–55.

[88] Mann GW, Madamadakala GR, Eckels SJ. Heat transfer characteristics of R-134a in a converging–diverging nozzle. Int J Heat Fluid Flow 2016;62(Pt B): 464–73.

[89] Liu B, Cai J, Huai X, Li F. Cavitation bubble collapse near a heated wall and its effect on the heat transfer. J Heat Transfer 2014;136(2):022901.

[90] Liu B, Cai J, Tao Y, Huai X. Interaction of two cavitation bubbles in a tube and its effects on heat transfer. J Therm Sci 2017;26(1):66–72.

[91] Mason TJ, Lorimer JP. Applied sonochemistry: the uses of power ultrasound in chemistry and processing. Weinheim: Wiley-VCH Verlag GmbH; 2002.

[92] Gogate PR, Kabadi AM. A review of applications of cavitation in biochemical engineering/biotechnology. Biochem Eng J 2009;44(1):60–72.

[93] Gogate PR, Sutkar VS, Pandit AB. Sonochemical reactors: important design and scale up considerations with a special emphasis on heterogeneous systems. Chem Eng J 2011;166(3):1066–82.

[94] Plesset MS, Prosperetti A. Bubble dynamics and cavitation. Annu Rev Fluid Mech 1977;9:145–85.

[95] Peng K, Tian S, Li G, Huang Z, Yang R, Guo Z. Bubble dynamics characteristics and influencing factors on the cavitation collapse intensity for self-resonating cavitating jets. Pet Explor Dev 2018;45(2):343–50.

[96] Karamah EF, Bismo S, Purwanto WW. Significance of acoustic and hydrodynamic cavitations in enhancing ozone mass transfer. Ozone Sci Eng 2013;35(6):482–8.

[97] Zhang H, Duan L, Zhang D. Absorption kinetics of ozone in water with ultrasonic radiation. Ultrason Sonochem 2007;14(5):552–6.

[98] Kelkar MA, Gogate PR, Pandit AB. Intensification of esterification of acids for synthesis of biodiesel using acoustic and hydrodynamic cavitation. Ultrason Sonochem 2008;15(3):188–94.

[99] Milly PJ, Toledo RT, Chen J, Kazem B. Hydrodynamic cavitation to improve bulk fluid to surface mass transfer in a nonimmersed ultraviolet system for minimal processing of opaque and transparent fluid foods. J Food Sci 2007; 72(9):M407–13.

[100] Chuah LF, Yusup S, Abd Aziz AR, Bokhari A, Abdullah MZ. Cleaner production of methyl ester using waste cooking oil derived from palm olein using a hydrodynamic cavitation reactor. J Clean Prod 2016;112(Pt 5):4505–14.

[101] Braeutigam P, Franke M, Schneider RJ, Lehmann A, Stolle A, Ondruschka B. Degradation of carbamazepine in environmentally relevant concentrations in water by hydrodynamic–acoustic–cavitation (HAC). Water Res 2012;46(7): 2469–77.

[102] Franke M, Braeutigam P, Wu ZL, Ren Y, Ondruschka B. Enhancement of chloroform degradation by the combination of hydrodynamic and acoustic cavitation. Ultrason Sonochem 2011;18(4):888–94.

[103] Arrojo S, Benito Y, Martínez TA. A parametrical study of disinfection with hydrodynamic cavitation. Ultrason Sonochem 2008;15(5):903–8.

[104] Gogate PR. Cavitational reactors for process intensification of chemical processing applications: a critical review. Chem Eng Process 2008;47(4): 515–27.

[105] Capocelli M, Prisciandaro M, Musmarra D, Lancia A. Understanding the physics of advanced oxidation in a venturi reactor. Chem Eng Trans 2013;32: 691–6.

[106] Moholkar VS, Pandit AB. Bubble behavior in hydrodynamic cavitation: effect of turbulence. AIChE J 1997;43(6):1641–8.

[107] Capocelli M, Prisciandaro M, Lancia A, Musmarra D. Modeling of cavitation as an advanced wastewater treatment. Desalination Water Treat 2013;51(7–9): 1609–14.

[108] Gogate PR, Pandit AB. Engineering design methods for cavitation reactors II: hydrodynamic cavitation. AIChE J 2000;46(8):1641–9.

[109] Gong C, Hart DP. Ultrasound induced cavitation and sonochemical yields. J Acoust Soc Am 1998;104(5):2675–82.

[110] Sochard S, Wilhelm AM, Delmas H. Modelling of free radicals production in a collapsing gas–vapour bubble. Ultrason Sonochem 1997;4(2):77–84.

[111] Gireesan S, Pandit AB. Modeling the effect of carbon-dioxide gas on cavitation. Ultrason Sonochem 2017;34:721–8.

[112] Fourest T, Deletombe E, Faucher V, Arrigoni M, Dupas J, Laurens JM. Comparison of Keller–Miksis model and finite element bubble dynamics simulations in a confined medium. Application to the hydrodynamic ram. Eur J Mech B 2018;68:66–75.

[113] Munter R. Advanced oxidation processes—current status and prospects. Proc Estonian Acad Sci Chem 2001;50(2):59–80.

[114] Badve M, Gogate P, Pandit A, Csoka L. Hydrodynamic cavitation as a novel approach for wastewater treatment in wood finishing industry. Separ Purif Tech 2013;106:15–21.

[115] Joshi SM, Gogate PR. Intensification of industrial wastewater treatment using hydrodynamic cavitation combined with advanced oxidation at operating capacity of 70 L. Ultrason Sonochem 2019;52:375–81.

[116] Bandala ER, Rodriguez-Narvaez OM. On the nature of hydrodynamic cavitation process and its application for the removal of water pollutants. Air Soil Water Res 2019;12:1178622119880488.

[117] Arrojo S, Nerín C, Benito Y. Application of salicylic acid dosimetry to evaluate hydrodynamic cavitation as an advanced oxidation process. Ultrason Sonochem 2007;14(3):343–9.

[118] Amin LP, Gogate PR, Burgess AE, Bremner DH. Optimization of a hydrodynamic cavitation reactor using salicylic acid dosimetry. Chem Eng J 2010;156(1):165–9.

[119] Zupanc M, Petkovšek M, Zevnik J, Kozmus G, Šmid A, Dular M. Anomalies detected during hydrodynamic cavitation when using salicylic acid dosimetry to measure radical production. Chem Eng J 2020;396:125389.

[120] Wang B, Su H, Zhang B. Hydrodynamic cavitation as a promising route for wastewater treatment—a review. Chem Eng J 2021;412:128685.

[121] Rajoriya S, Bargole S, Saharan VK. Degradation of a cationic dye (rhodamine 6G) using hydrodynamic cavitation coupled with other oxidative agents: reaction mechanism and pathway. Ultrason Sonochem 2017;34:183–94.

[122] Wang X, Wang J, Guo P, Guo W, Wang C. Degradation of rhodamine B in aqueous solution by using swirling jet-induced cavitation combined with H_2O_2. J Hazard Mater 2009;169(1–3):486–91.

[123] Wang X, Jia J, Wang Y. Combination of photocatalysis with hydrodynamic cavitation for degradation of tetracycline. Chem Eng J 2017;315:274–82.

[124] Li P, Song Y, Yu S. Removal of Microcystis aeruginosa using hydrodynamic cavitation: performance and mechanisms. Water Res 2014;62:241–8.

[125] Rajak U, Verma TN. Effect of emission from ethylic biodiesel of edible and non-edible vegetable oil, animal fats, waste oil and alcohol in CI engine. Energy Convers Manage 2018;166:704–18.

[126] Farvardin M, Samani BH, Rostami S, Abbaszadeh-Mayvan A, Najafi G, Fayyazi E. Enhancement of biodiesel production from waste cooking oil: ultrasonic–hydrodynamic combined cavitation system. Energ Source Part A 2022;44(2):5065–79.

[127] Samani BH, Behruzian M, Najafi G, Fayyazi E, Ghobadian B, Behruzian A, et al. The rotor–stator type hydrodynamic cavitation reactor approach for enhanced biodiesel fuel production. Fuel 2021;283:118821.

[128] Mohod AV, Gogate PR, Viel G, Firmino P, Giudici R. Intensification of biodiesel production using hydrodynamic cavitation based on high speed homogenizer. Chem Eng J 2017;316:751–7.

[129] Innocenzi V, Prisciandaro M. Technical feasibility of biodiesel production from virgin oil and waste cooking oil: comparison between traditional and innovative process based on hydrodynamic cavitation. Waste Manag 2021;122:15–25.

[130] Chuah LF, Klemeš JJ, Yusup S, Bokhari A, Akbar MM, Chong ZK. Kinetic studies on waste cooking oil into biodiesel via hydrodynamic cavitation. J Clean Prod 2017;146:47–56.

[131] Grillo G, Boffa L, Binello A, Mantegna S, Cravotto G, Chemat F, et al. Cocoa bean shell waste valorisation; extraction from lab to pilot-scale cavitational reactors. Food Res Int 2019;115:200–8.

[132] Albanese L, Bonetti A, D'Acqui LP, Meneguzzo F, Zabini F. Affordable production of antioxidant aqueous solutions by hydrodynamic cavitation processing of silver fir (Abies alba Mill.) needles. Foods 2019;8(2):65.

[133] Preece KE, Hooshyar N, Krijgsman AJ, Fryer PJ, Zuidam NJ. Intensification of protein extraction from soybean processing materials using hydrodynamic cavitation. Innov Food Sci Emerg Technol 2017;41:47–55.

[134] Lee I, Han JI. Simultaneous treatment (cell disruption and lipid extraction) of wet microalgae using hydrodynamic cavitation for enhancing the lipid yield. Bioresour Technol 2015;186:246–51.

[135] Setyawan M, Budiman A, Mulyono P. Optimum extraction of algae-oil from microalgae using hydrodynamic cavitation. Int J Renew Energ Res 2018;8(1):451–8.

[136] Tabatabaei M, Aghbashlo M, Dehhaghi M, Panahi HKS, Mollahosseini A, Hosseini M, et al. Reactor technologies for biodiesel production and processing: a review. Pror Energy Combust Sci 2019;74:239–303.

[137] Zhang Z, Wang G, Nie Y, Ji J. Hydrodynamic cavitation as an efficient method for the formation of sub-100 nm O/W emulsions with high stability. Chin J Chem Eng 2016;24(10):1477–80.

[138] Moholkar VS, Pandit AB. Modeling of hydrodynamic cavitation reactors: a unified approach. Chem Eng Sci 2001;56(21–22):6295–302.

[139] Ozonek J. Application of hydrodynamic cavitation in environmental engineering. London: CRC Press; 2012.

[140] Lunnbäck J. Hydrodynamic cavitation applied to anaerobic degradation of fats, oils and greases (FOGs) [dissertation]. Linköping: Linköping University; 2016.

[141] Carpenter J, Badve M, Rajoriya S, George S, Saharan VK, Pandit AB. Hydrodynamic cavitation: an emerging technology for the intensification of various chemical and physical processes in a chemical process industry. Rev Chem Eng 2016;33(5):433–68.

[142] Arrojo S, Benito Y. A theoretical study of hydrodynamic cavitation. Ultrason Sonochem 2008;15(3):203–11.

[143] Sharma A, Gogate PR, Mahulkar A, Pandit AB. Modeling of hydrodynamic cavitation reactors based on orifice plates considering hydrodynamics and chemical reactions occurring in bubble. Chem Eng J 2008;143(1–3):201–9.

[144] Vichare NP, Gogate PR, Pandit AB. Optimization of hydrodynamic cavitation using a model reaction. Chem Eng Technol 2000;23(8):683–90.

[145] Ai W, Ding T. Orifice plate cavitation mechanism and its influencing factors. Water Sci Eng 2010;3(3):321–30.

[146] Simpson A, Ranade VV. Modelling of hydrodynamic cavitation with orifice: influence of different orifice designs. Chem Eng Res Des 2018;136:698–711.

[147] Ghayal D, Pandit AB, Rathod VK. Optimization of biodiesel production in a hydrodynamic cavitation reactor using used frying oil. Ultrason Sonochem 2013;20(1):322–8.

[148] Huang Y, Wu Y, Huang W, Yang F, Ren X. Degradation of chitosan by hydrodynamic cavitation. Polym Degrad Stabil 2013;98(1):37–43.

[149] Sivakumar M, Pandit AB. Wastewater treatment: a novel energy efficient hydrodynamic cavitational technique. Ultrason Sonochem 2002;9(3):123–31.

[150] Rudolf P, Kubina D, Hudec M, Kozák J, Maršálek B, Maršálková E, et al. Experimental investigation of hydrodynamic cavitation through orifices of different geometries. EPJ Web Conf 2017;143:143.

[151] Senthil Kumar P, Siva Kumar M, Pandit AB. Experimental quantification of chemical effects of hydrodynamic cavitation. Chem Eng Sci 2000;55(9):1633–9.

[152] Kalumuck KM, Chahine GL. The use of cavitating jets to oxidize organic compounds in water. J Fluids Eng 2000;122(3):465–70.

[153] Bagade VS, Suryawanshi PM, Nalavade SM. A review of multi-hole orifice plate. Int J Res Appl Sci Eng Technol 2019;7(4):3197–208.

[154] Saharan VK, Rizwani MA, Malani AA, Pandit AB. Effect of geometry of hydrodynamically cavitating device on degradation of orange-G. Ultrason Sonochem 2013;20(1):345–53.

[155] Panda D, Saharan VK, Manickam S. Controlled hydrodynamic cavitation: a review of recent advances and perspectives for greener processing. Processes 2020;8(2):220.

[156] Bashir TA, Soni AG, Mahulkar AV, Pandit AB. The CFD driven optimisation of a modified venturi for cavitational activity. Can J Chem Eng 2011;89(6):1366–75.

[157] Ulas A. Passive flow control in liquid-propellant rocket engines with cavitating venturi. Flow Meas Instrum 2006;17(2):93–7.

[158] Ashrafizadeh SM, Ghassemi H. Experimental and numerical investigation on the performance of small-sized cavitating venturis. Flow Meas Instrum 2015;42:6–15.

[159] Brinkhorst S, von Lavante E, Wendt G. Numerical investigation of effects of geometry on cavitation in Herschel Venturi-tubes applied to liquid flow metering. In: Proceeding of the 9th International Symposium of Fluid Flow Measurement Publications; 2015 Apr 14–17; Arlington, VA, USA; 2015.

[160] Li M, Bussonnière A, Bronson M, Xu Z, Liu Q. Study of venturi tube geometry on the hydrodynamic cavitation for the generation of microbubbles. Miner Eng 2019;132:268–74.

[161] Bimestre TA, Júnior JAM, Botura CA, Canettieri E, Tuna CE. Theoretical modeling and experimental validation of hydrodynamic cavitation reactor with a venturi tube for sugarcane bagasse pretreatment. Bioresour Technol 2020;311:123540.

[162] Kuldeep, Saharan VK. Computational study of different venturi and orifice type hydrodynamic cavitating devices. J Hydrodyn Ser B 2016;28(2):293–305.

[163] Franc JP, Michel JM. Fundamentals of cavitation. Dordrecht: Springe; 2005.

[164] Kim H, Koo B, Lee S, Yoon JY. Experimental study of cavitation intensity using a novel hydrodynamic cavitation reactor. J Mech Sci Technol 2019;33(9):4303–10.

[165] Jyoti KK, Pandit AB. Water disinfection by acoustic and hydrodynamic cavitation. Biochem Eng J 2001;7(3):201–12.

[166] Sun X, Kang CH, Park JJ, Kim HS, Om AS, Yoon JY. An experimental study on the thermal performance of a novel hydrodynamic cavitation reactor. Exp Therm Fluid Sci 2018;99:200–10.

[167] Šarc A, Oder M, Dular M. Can rapid pressure decrease induced by supercavitation efficiently eradicate Legionella pneumophila bacteria? Desalin Water Treat 2016;57(5):2184–94.

[168] Crudo D, Bosco V, Cavaglià G, Grillo G, Mantegna S, Cravotto G. Biodiesel production process intensification using a rotor–stator type generator of hydrodynamic cavitation. Ultrason Sonochem 2016;33:220–5.

[169] Maršálek B, Zezulka Š, Maršálková E, Pochylý F, Rudolf P. Synergistic effects of trace concentrations of hydrogen peroxide used in a novel hydrodynamic cavitation device allows for selective removal of cyanobacteria. Chem Eng J 2020;382:122383.

[170] Patil PN, Gogate PR, Csoka L, Dregelyi-Kiss A, Horvath M. Intensification of biogas production using pretreatment based on hydrodynamic cavitation. Ultrason Sonochem 2016;30:79–86.

[171] Šarc A, Kosel J, Stopar D, Oder M, Dular M. Removal of bacteria *Legionella pneumophila*, *Escherichia coli*, and *Bacillus subtilis* by (super)cavitation. Ultrason Sonochem 2018;42:228–36.

[172] Loraine G, Chahine G, Hsiao CT, Choi JK, Aley P. Disinfection of Gram-negative and Gram-positive bacteria using DynaJets® hydrodynamic cavitating jets. Ultrason Sonochem 2012;19(3):710–7.

[173] Sun X, Jia X, Liu J, Wang G, Zhao S, Ji L, et al. Investigation on the characteristics of an advanced rotational hydrodynamic cavitation reactor for water treatment. Sep Purif Technol 2020;251:117252.

[174] Cerecedo LM, Dopazo C, Gomez-Lus R. Water disinfection by hydrodynamic cavitation in a rotor–stator device. Ultrason Sonochem 2018;48:71–8.

[175] Kosel J, Šuštaršič M, Petkovšek M, Zupanc M, Sežun M, Dular M. Application of (super)cavitation for the recycling of process waters in paper producing industry. Ultrason Sonochem 2020;64:105002.

[176] Zupanc M, Kosjek T, Petkovšek M, Dular M, Kompare B, Širok B, et al. Shear-induced hydrodynamic cavitation as a tool for pharmaceutical micropollutants removal from urban wastewater. Ultrason Sonochem 2014;21(3):1213–21.

[177] Vilarroig J, Martínez R, Zuriaga-Agustí E, Torró S, Galián M, Chiva S. Design and optimization of a semi-industrial cavitation device for a pretreatment of an anaerobic digestion treatment of excess sludge and pig slurry. Water Environ Res 2020;92(12):2060–71.

[178] Kosel J, Šinkovec A, Dular M. A novel rotation generator of hydrodynamic cavitation for the fibrillation of long conifer fibers in paper production. Ultrason Sonochem 2019;59:104721.

[179] Petkovšek M, Mlakar M, Levstek M, Stražar M, Širok B, Dular M. A novel rotation generator of hydrodynamic cavitation for waste-activated sludge disintegration. Ultrason Sonochem 2015;26:408–14.

[180] Sežun M, Kosel J, Zupanc M, Hočevar M, Vrtovšek J, Petkovšek M, et al. Cavitation as a potential technology for wastewater management—an example of enhanced nutrient release from secondary pulp and paper mill sludge. Stroj Vestn-J Mech Eng 2019;65(11–12):641–9.

[181] Kovačič A, Škufca D, Zupanc M, Gostiša J, Bizjan B, Krištofelc N, et al. The removal of bisphenols and other contaminants of emerging concern by hydrodynamic cavitation: from lab-scale to pilot-scale. Sci Total Environ 2020;743:140724.

[182] Dular M, Griessler-Bulc T, Gutierrez-Aguirre I, Heath E, Kosjek T, Krivograd Klemenčič A, et al. Use of hydrodynamic cavitation in (waste)water treatment. Ultrason Sonochem 2016;29:577–88.

[183] Ranade VV, Kulkarni AA, Bhandari VM, inventors; Council of Scientific & Industrial Research (New Delhi, IN), assignee. Vortex diodes as effluent treatment devices. United States Patent 9422952. 2016 Aug 23.

[184] Jain P, Bhandari VM, Balapure K, Jena J, Ranade VV, Killedar DJ. Hydrodynamic cavitation using vortex diode: an efficient approach for elimination of pathogenic bacteria from water. J Environ Manage 2019;242:210–9.

[185] Gaikwad V, Ranade V. Disinfection of water using vortex diode as hydrodynamic cavitation reactor. Asian J Chem 2016;28(8):1867–70.

[186] Suryawanshi NB, Bhandari VM, Sorokhaibam LG, Ranade VV. A non-catalytic deep desulphurization process using hydrodynamic cavitation. Sci Rep 2016;6(1):33021.